PRECISION EQUIPMENT FOR MEASUREMENTS ON A DOUBLE-STREAM MICROWAVE AMPLIFIER TUBE.

by

Clarence Robert Crowell.

A Thesis submitted to the Faculty of Graduate Studies and Research at McGill University in partial fulfilment of the requirements of the degree of Master of Science.

Eaton Research Laboratory,
McGill University.

August 1951.

TABLE OF CONTENTS

TABLE OF CONTENTS (Cont'd.)

PAGE

PART TWO

DOUBLE-STREAM MICROWAVE AMPLIFICATION

ABSTRACT

The design and construction of a microwave signal generator have been discussed. A 10 cm. signal generator has been built and the absolute available output power of the signal generator has been precisely calibrated. This involved calibrating a cutoff attenuator which controlled the power output, and a measurement of the absolute available output power at low attenuation. This calibration enabled the signal generator to be used for signal and noise measurements on a double-stream microwave amplifier tube.

The theory of double-stream amplification has been reviewed and the construction of double-stream amplifier tubes discussed. The output of an experimental double-stream amplifier tube was examined at a signal wavelength of 10.7 cm. The observations revealed the existence of double-stream amplification.

INTRODUCTION

Double-stream amplification is a recently developed method for amplifying radio frequency signals. The initial work on double-stream amplification was done by J.R. Pierce and A.V. Haeff. It was predicted that if the current densities and average velocities of two electron streams fulfilled certain conditions, velocity modulation of the beams could set up a growing space charge wave in the electron streams. The conditions to be satisfied are considered in Part Two of this thesis.

Double-stream amplification has been observed by A.V. Haeff (1) at 3000 megacycles per second and by A.V. Hollenberg (2) at 255 megacycles per second. Theoretical treatments have been published by L.S. Nergaard (3) and J.R. Pierce and W.B. Hebenstreit (4). Pierce has also published two further papers (5) and (6) dealing with the design of double-stream amplifiers.

This thesis describes a portion of the work done in the course of an investigation of double-stream amplification. The author was responsible for constructing and calibrating the equipment necessary to evaluate the performance of a double-stream amplifier tube designed to operate at 2800 megacycles per second. The design and construction of the double-stream amplifier tube were carried out by G.A. Harrower. The measurements of the behaviour of the tube were made jointly by Mr. Harrower and the author. The objective of the research was to obtain evidence of double-stream amplification. The measuring equipment was also designed so that the noise figure of a double-stream amplifier could be measured. The work described

in this thesis therefore falls into two categories. The construction and calibration of the measuring equipment is treated in Part One. The work dealing directly with double-stream amplification is discussed in Part Two.

PART ONE

THE CONSTRUCTION AND PRECISION CALIBRATION OF EQUIPMENT FOR MAKING SIGNAL AND NOISE MEASUREMENTS IN THE NEIGHBORHOOD OF 10 CM.

I SIGNAL AND NOISE MEASUREMENTS

Before describing the necessary equipment, terms used in signal and noise measurements will be defined and methods of taking measurements outlined. This will reveal some of the requirements to be fulfilled by the measuring equipment. The following paragraphs lead up to a definition of noise figure in terms of available power, gain, and effective bandwidth. The treatment is similar to that presented in articles by H.T. Friis (7) and G.A. Woonton (8), and Sections 4.1 and 4.2 of reference (9), but combines aspects not common to all three.

Available Signal Power.

Available signal power is the maximum power a signal source can deliver. The power delivered to an impedance R_1 ohms by a generator with an electromotive force E volts and internal impedance R_o ohms is $E^2R_1/(R_o+R_1)^2$ watts. This power has a maximum value $E^2/4R_o$ when R_1 equals R_o. The available signal power from the generator is therefore $E^2/4R_o$. The available signal power from a signal source is defined in such a way that its value is independent of the load impedance.

If it is desired to connect a source of known available signal power to the input of a network, the available output power of the signal source must have been found by a calibration process or calculated absolutely. A signal generator is a

source which satisfies this requirement. It will be assumed therefore that measurements will be made with a signal generator connected at the input of the network under test. The available output power of a network can be measured with a receiver calibrated to read delivered power, but matched for maximum power transfer.

Gain.

The gain of a four terminal network is the ratio of the available signal power at the output terminals of the network to the available signal power of the signal generator at the input terminals. The gain of a network depends on the impedance matching at the input, but not on that at the output. The internal impedance of the signal generator therefore affects the gain of a network.

Available Noise Power.

The available noise power between two terminals of a network is the noise power which would be delivered to an output circuit matched for maximum power transfer. The available noise power at the output of a network is due to all the noise generated inside the network plus the noise generated in the signal generator at the input of the network.

Any resistor is a source of Johnson noise, an important source of noise in signal generators used to measure noise figures. The energy associated with this noise is uniformly distributed over the whole frequency spectrum. Between the frequencies f and $f + \Delta f$, the available Johnson noise power at the output of a signal generator is

$$\Delta j = k T \Delta f \qquad (1)$$

where k is Boltzmann's constant and T is the absolute temperature of the internal impedance of the signal generator. T is usually considered to be 300° K. If G(f) is the gain of a network at the frequency f, the available Johnson noise power at the input of the network produces an available output noise power

$$J = \int_0^\infty kTG(f)df = kT\int_0^\infty G(f)df \qquad (2)$$

from the whole acceptance band of the network.

The available noise power N at the output of a network can be measured by finding the single frequency signal power equivalent to it. If s(N) is the input signal power which makes the total output power twice that with only noise in the output circuit,

$$N = G(f)s(N). \qquad (3)$$

This equation is valid whether or not the output power indicator is matched to the network.

Effective Bandwidth.

The effective or noise bandwidth of a network is

$$B = \int_0^\infty G(f)df/G(f_o), \qquad (4)$$

where f_o is the frequency at which the network gain is a maximum. The effective bandwidth of a network can be found graphically from its frequency response curve.

Equations (2) and (4) can be combined to give an alternative expression for J :

$$J = kTBG(f_o). \qquad (5)$$

This is also the noise power which would be available at the output if the network had a gain $G(f_o)$ over a frequency range

of width B, and no response at other frequencies.

Noise Figure.

The noise figure of a network between the frequencies f and $f + \Delta f$ is the ratio of the available signal power to available noise power ratio at the input of the network to that at the output. Hence the noise figure is given by

$$F(f) = (s/\Delta n)/(S/\Delta N), \tag{6}$$

where s and S are the input and output available signal powers at the frequency f and Δn and ΔN the available input and output noise powers between the frequencies f and $f + \Delta f$. Since

$$S/s = G(f),$$
$$F(f) = N/G(f)\Delta n \ . \tag{7}$$

$G(f)\Delta n$ is the available output noise power arising from noise in the signal generator. This means that the noise figure can be alternately defined as the ratio of the total available output noise power to the available output noise power caused by noise generated in the signal generator.

The effective noise figure or the noise figure averaged with respect to network gain over the acceptance band of the network is

$$\overline{F} = \int_{\cdot}^{\infty} F(f)G(f)df \Big/ \int_{\cdot}^{\infty} G(f)df. \tag{8}$$

$\overline{F}$ is of greater experimental use than F because $\overline{F}$ refers to the response of the network as a whole.

If the input noise Δn in equation (7) is solely Johnson noise, it follows from equation (1) that

$$\Delta N = F(f)G(f)k\,T\Delta f \ , \tag{9}$$

and the total noise output power available over the band-pass of the network is

$$N = kT\int_{0}^{\infty} F(f)G(f)df \ . \qquad (10)$$

From the definitions of B (equation 4) and $\overline{F}$ (equation 8), it follows that

$$\overline{F} = N/(kTBG(f_o)) \ . \qquad (11)$$

If the output noise power of the network is measured at a frequency f_o, as in equation 3, equation 11 becomes

$$\overline{F} = s(N)/(kTB). \qquad (12)$$

To evaluate $\overline{F}$ from equation 12, the device measuring the output power must have a uniform response over the band-pass of the network and generate no noise within itself. If the output power is measured with a superheterodyne receiver, the frequency response and output noise power of the system as a whole are determined by the band-pass of the i.f. amplifier in the receiver. The B in equation 12 must then be the effective bandwidth of the i.f. amplifier. Error due to noise in the receiver may be eliminated by using the relation

$$F_n = F_{n+r} - (F_r-1)/G_n \ , \qquad (13)$$

where F_n is the noise figure of the network, F_r the noise figure of the receiver, F_{n+r} the noise figure of the network and receiver in series, and G_n the gain of the network. This relationship is a particular case of a more general one derived in reference (8). The correction involving the noise figure of the receiver should not be very important in measuring the

noise figure of an amplifier, since any practical amplifier must have an appreciable gain.

When giving a measured value of the noise figure of a network, it is customary to specify the internal impedance of the signal generator used in the measurement, and the impedance matching at the input of the network. Both affect the value of the noise figure. The internal impedance of the signal generator should be the same as that of the signal source used in the application of the network. This is important because the gain and the output noise power of the network depend on the signal source impedance. The impedance matching at the input of a network also affects the noise figure. Maximum gain does not necessarily imply minimum noise figure. A slight mismatch may cause a greater decrease in output noise power than in the gain of the network and thus improve the noise figure. The latter is usually quoted for a circuit adjusted either for maximum power transfer or for minimum noise figure.

II THE CONSTRUCTION OF A MICROWAVE SIGNAL GENERATOR

The methods of measuring the quantities previously described require a signal generator to supply signals of known absolute power, a microwave receiver to measure output power, and a wavemeter to measure microwave frequencies. A signal generator was built and calibrated for this purpose.

Design Requirements

If a signal generator is to be satisfactory for signal and noise measurements, it must deliver a stable signal of known absolute available power, frequency, and modulation characteristics, and have a known internal impedance. These

four considerations are discussed in the following paragraphs. Design requirements are considered only for the type of signal generator consisting essentially of a microwave oscillator delivering signal power through a variable attenuator.

Signal Power.

The signal power required can be as low as 10^{-12} watts if the signal generator is to be used for noise measurements made with receiving systems having small bandwidths (see equation 12). A c.w. microwave oscillator cannot produce signals at such a low level without using an attenuator. Direct absolute measurement of power output lower than a few microwatts is also not feasible. This measurement problem can be avoided by sending the oscillator output through a calibrated variable attenuator and measuring the absolute output power at low attenuation. The output power at high attenuation can then be calculated. The oscillator output power must be of the order of milliwatts to permit an absolute measurement. A disadvantage of this system is the fact that the oscillator shielding must be very carefully designed. Since the smallest signal power desired may be about 100 decibels below the oscillator output, the oscillator shielding may have to furnish 130 or more decibels protection against leakage from the oscillator. The protection necessary depends critically on the accuracy desired in the measurements. Sections 4.9 and 13.5 of reference (9) contain a description of the way in which errors may be caused by leakage, and the size of the errors involved.

Frequency.

For signal and noise measurements it is not as important for the frequency of a signal generator to be known accurately as it is for the frequency to be stable. Frequency stability is important because many components in an r.f. circuit require matching adjustments which are frequency dependent. Frequency stability is of still greater importance if the power output is measured with a superheterodyne receiver. This is because the bandwidth of the i.f. amplifier in a receiver is usually narrow in comparison with small frequency changes in the r.f. signal.

Modulation.

A signal generator should be designed so that several types of modulation are available. This allows the signal generator to simulate signals from different types of equipment and permits the use of different detecting systems. C.w. output is desirable when the detector is a superheterodyne receiver or a bolometer in a bridge for absolute power measurement. Audio-frequency modulation is necessary when the detector is a crystal or bolometer in the input of an audio amplifier. Square-wave or pulse modulation is usually desirable in this case. Frequency modulation can be used to sweep the signal output over the acceptance band of the receiving system. The frequency response of the receiver can then be obtained if the output is displayed on an oscilloscope. This can be very useful for measuring the noise bandwidth of networks which have bandwidths over which the oscillator output power is constant.

Internal Impedance.

The internal impedance of a signal generator must have the same value as that of the signal source which will replace it in practice. It is difficult to construct variable r.f. attenuators which will have a desired internal impedance. The signal generator can be given the required internal impedance if a fixed attenuator of the desired output impedance and about 10 decibels attenuation is placed at the output of the variable attenuator. Large changes in the output impedance of the variable attenuator then produce small and relatively unimportant changes in the effective internal impedance of the signal generator.

Details of Construction

A signal generator was built using as a guide a description in Section 4.12 of reference (9). This signal generator was designed to provide an output of c.w., pulse modulated c.w., frequency-modulated, or amplitude-modulated power at wavelengths from 8.2 to 12.8 cm.

The Oscillator

The oscillator tube used was a McNally (707B) reflex klystron. The external portion of its cavity resonator was attached to copper disc seals through the tube walls. This resonant cavity was incorporated into a shielded tube mounting. Joints and threaded portions of the shield were tightly fitted and silver plated to prevent r.f. leakage. Leads to the tube passed through polyiron chokes which produced high attenuation of r.f. power. The resonant frequency of the cavity could be adjusted by two similar plungers, one

driven by a micrometer and the other, for coarse tuning, equipped with a setscrew. Two settings of the coarse tuning plunger were required to cover the complete range of cavity tuning. Figure II shows the variation of the resonant frequency of the cavity as the plunger settings were adjusted. These curves give only an approximate frequency calibration of the oscillator. This is because the operating frequency of a reflex klystron is also a function of the d.c. voltages applied to the klystron electrodes. Signal power was extracted from the oscillator cavity through a rectangular iris. This coupling excited the TE modes in a cutoff attenuator connected at the output of the oscillator.

The Cutoff Attenuator

The cutoff attenuator consisted of a precisely made length of circular waveguide one-half inch in diameter through which the oscillator output power had to pass. This waveguide was well beyond cutoff over the frequency range of the oscillator. Power was coupled from the guide by a movable coupling loop connected to a coaxial output cable. (See Figure III). The position of the loop in the guide was precisely controlled by the setting of a vernier dial on the front panel of the signal generator. The rectangular iris in the oscillator cavity and the output loop in the attenuator were designed to couple the TE_{11} mode in the waveguide in preference to TM modes. The attenuation of a signal propagated in a single mode in a waveguide beyond cutoff is

$$A = 8.686\, S_{mn}\, (1-(L_c/L)^2)^{\frac{1}{2}}/(rk_e^{\frac{1}{2}}) \qquad (14)$$

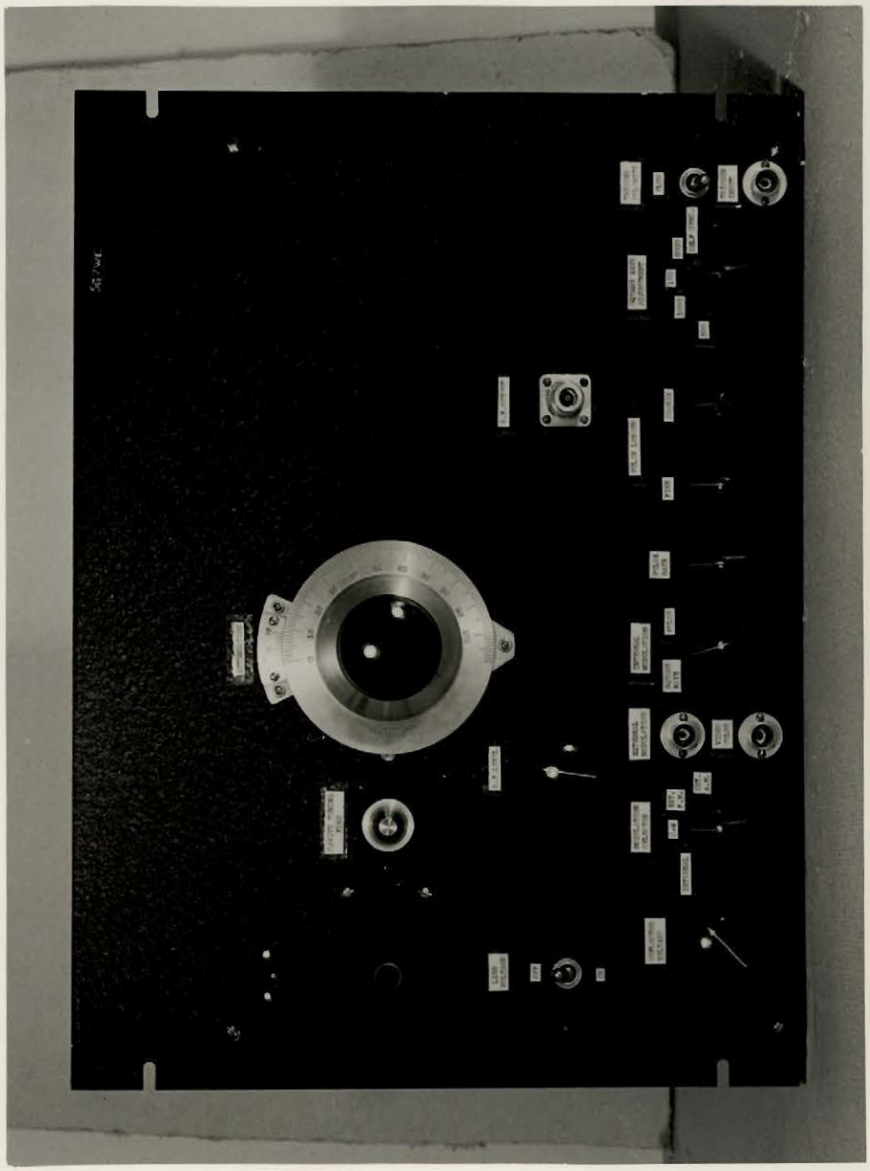

Figure 1
Signal Generator

Figure II
Frequency Calibration of
Signal Generator

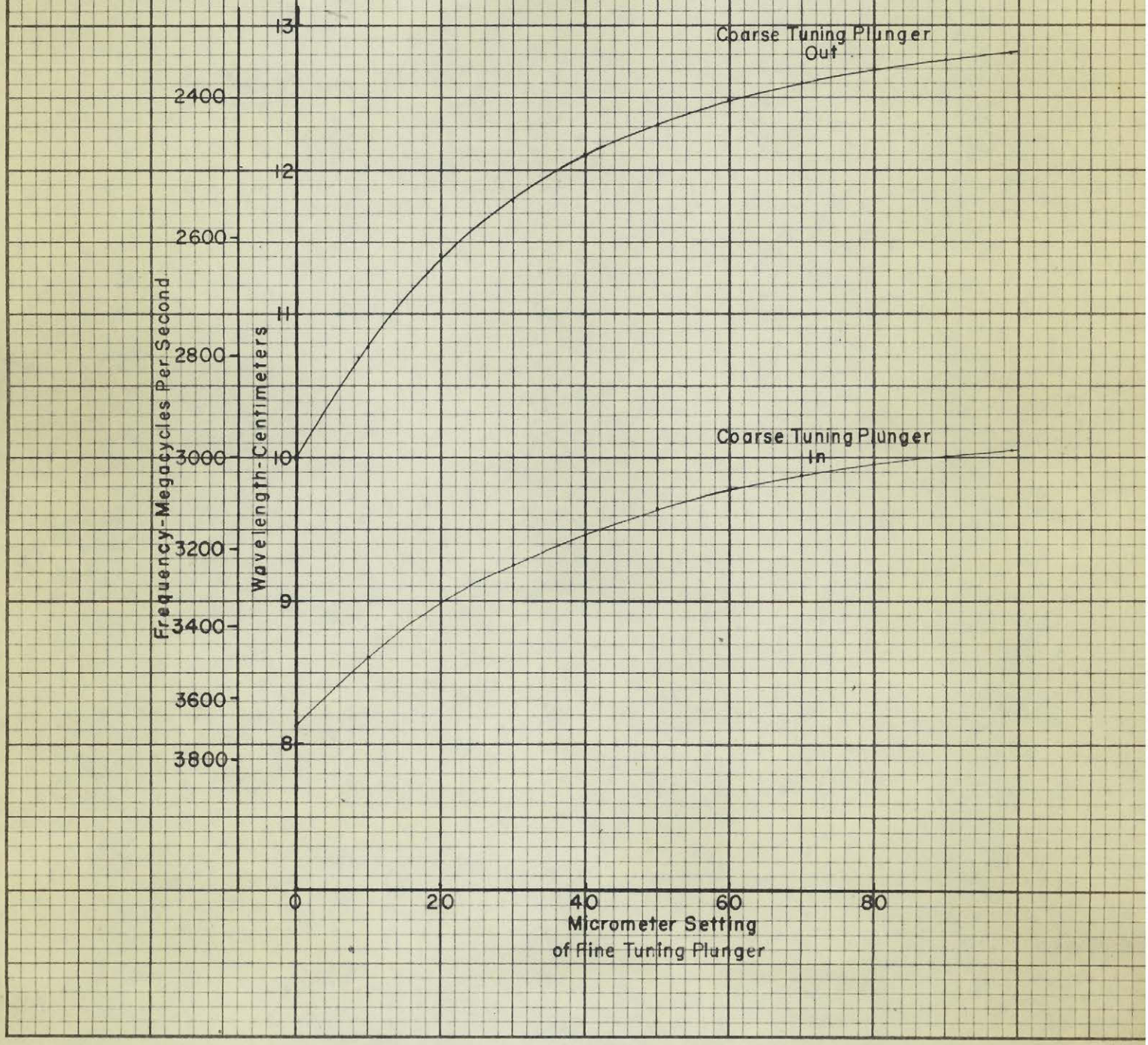

Figure III

Simplified Diagram of a Cutoff

Attenuator

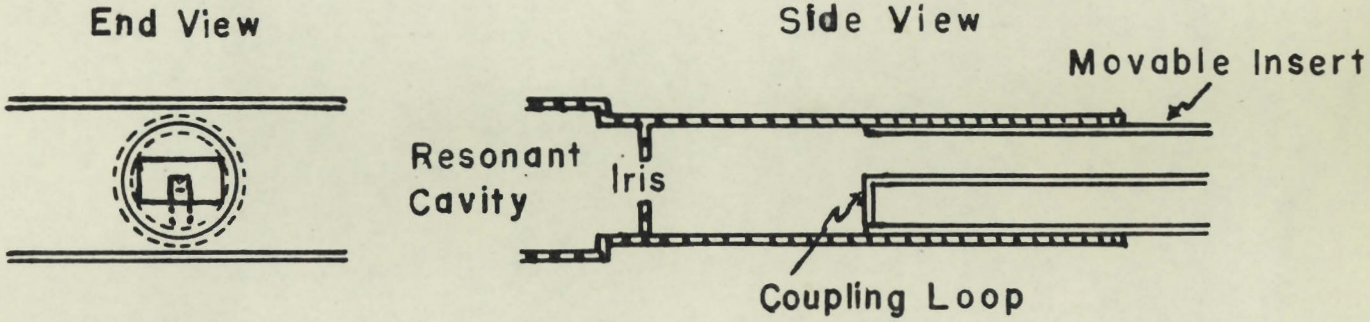

decibels per unit length. S_{mn} is a number characteristic of the mode, r the radius of the waveguide, k_e the relative dielectric constant, L the free space wavelength of the signal, and L_c the cutoff wavelength. ($L_c = 2 r k_e^{\frac{1}{2}} / S_{mn}$). Equation 14 is valid if L exceeds L_c by more than 5% and if the guide walls are infinitely conducting. This equation is derived in reference (10). The smallest S_{mn} is S_{11} for the TE_{11} mode. $S_{11} = 1.845$. All other modes have larger values of S_{mn} and thus experience more attenuation. Since the attenuator used also coupled the TE_{11} mode preferentially, such an attenuator would be expected to act as if only one mode were present. The attenuation would then vary directly with the displacement of the coupling loop. In practice when the coupling loop and iris are close together, there is always some coupling of other modes or a variation in the input impedance of the attenuator as the loop position is changed. Either of these effects can produce deviations from the behaviour predicted by equation 14. It is therefore necessary to calibrate a cutoff attenuator to determine the effect of these other factors.

D.C. and Audio-frequency Circuits

A block circuit diagram of the signal generator is shown in Figure IV, and a schematic diagram in Figure V. Much attention was given to voltage regulation in the circuit because the operating frequency of a klystron depends critically on the voltages applied to its reflector and accelerating grid. This property of klystrons was also of benefit, for it was used to obtain modulation of the output.

Figure 4
Block Diagram of Signal Generator

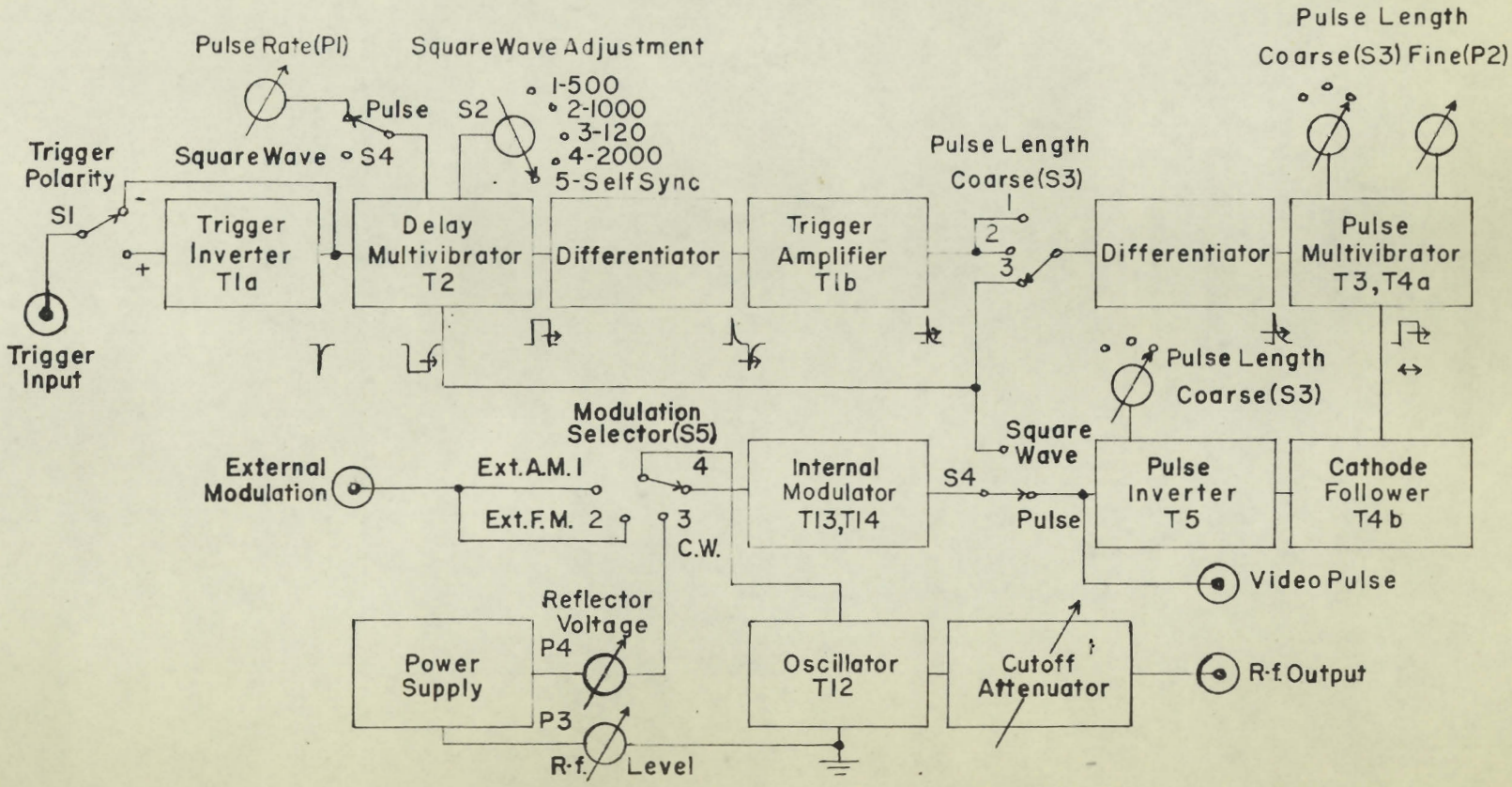

LEGEND FOR FIGURE V

RESISTORS

Symbol	Value	Wattage	Symbol	Value	Wattage	Symbol	Value	Wattage
R1	10K	1/2	R17	27K	1/2	R33	100K	1
R2	22K	2	R18	1K	2	R34	100K	1
R3	10K	2	R19	56K	1/2	R35	1M	1
R4	50K	1	R20	100K	1/2	R36	1K	10
R5	10K	2	R21	5.6K	1	R37	270K	1/2
R6	5.1K	2	R22	470K	1/2	R38	1.1K	2
R7	100K	1/2	R23	100K	1/2	R39	100	1/2
R8	10K	1/2	R24	22K	2	R40	100K	1/2
R9	1.5M	1/2	R25	560	1	R41	6K	20
R10	680K	1/2	R26	1.5K	1/2	R42	4K	20
R11	6.2M	1/2	R27	39K	2	P1	0-1.0M	1
R12	390K	1/2	R28	270K	1	P2	0-1.0M	1
R13	470K	1/2	R29	1K	1	P3	0-5K	25
R14	4.7K	1/2	R30	1K	1	P4	0-3.5K	25
R15	1.2M	1/2	R31	100	1/2	P5	50K	1
R16	100K	1/2	R32	100	1/2	P6	50K	1

CONDENSERS

Symbol	Value	Symbol	Value	Symbol	Value	Symbol	Value
C1	.01mf	C9	25mmf	C16	.01mf	C23	1mf
C2	.001mf	C10	25mmf	C17	4mf	C24	.1mf
C3	100mmf	C11	150mmf	C18	4mf	C25	.25mf
C4	250mmf	C12	.1mf	C19	.01mf	C26	1mf
C5	.25mf	C13	.1mf	C20	.1mf	C27	20mf
C6	100mmf	C14	300mmf	C21	.01mf	C28	.01mf
C7	25mmf	C15	4mf	C22	12mf	C29	8mf
C8	25mmf						

SWITCHES

Symbol	Type	Function
S1	S.P.D.T.	Trigger Polarity Switch.
S2	2 circuit 5 position selector.	Square Wave Adjustment.
S3	4 " 3 " "	Pulse Length Adjustment (coarse).
S4	2 " 2 " "	Pulse-Square Wave Selector.
S5	3 " 4 " "	Modulation Selector.
S6	D.P.D.T.	Line Voltage On-Off Switch.

TRANSFORMERS

Symbol		Description
H1,H2	Hammond H1128X60	Filament Transformer.
H3	Stangor 4STC44	High Voltage Transformer.

LEGEND FOR FIGURE V (Cont'd.)

CHOKES

Symbol	Value	Type
L1	1mh	
L2	1mh	
L3	.05mh	
L4	30h	Hammond 30-150X.

MISCELLANEOUS

Symbol	Description
F1	3 Ampere Fuse.
F2	1/16 Ampere Fuse.
J1, J2	Jones Plug.

FIGURE V

CIRCUIT OF SIGNAL GENERATOR

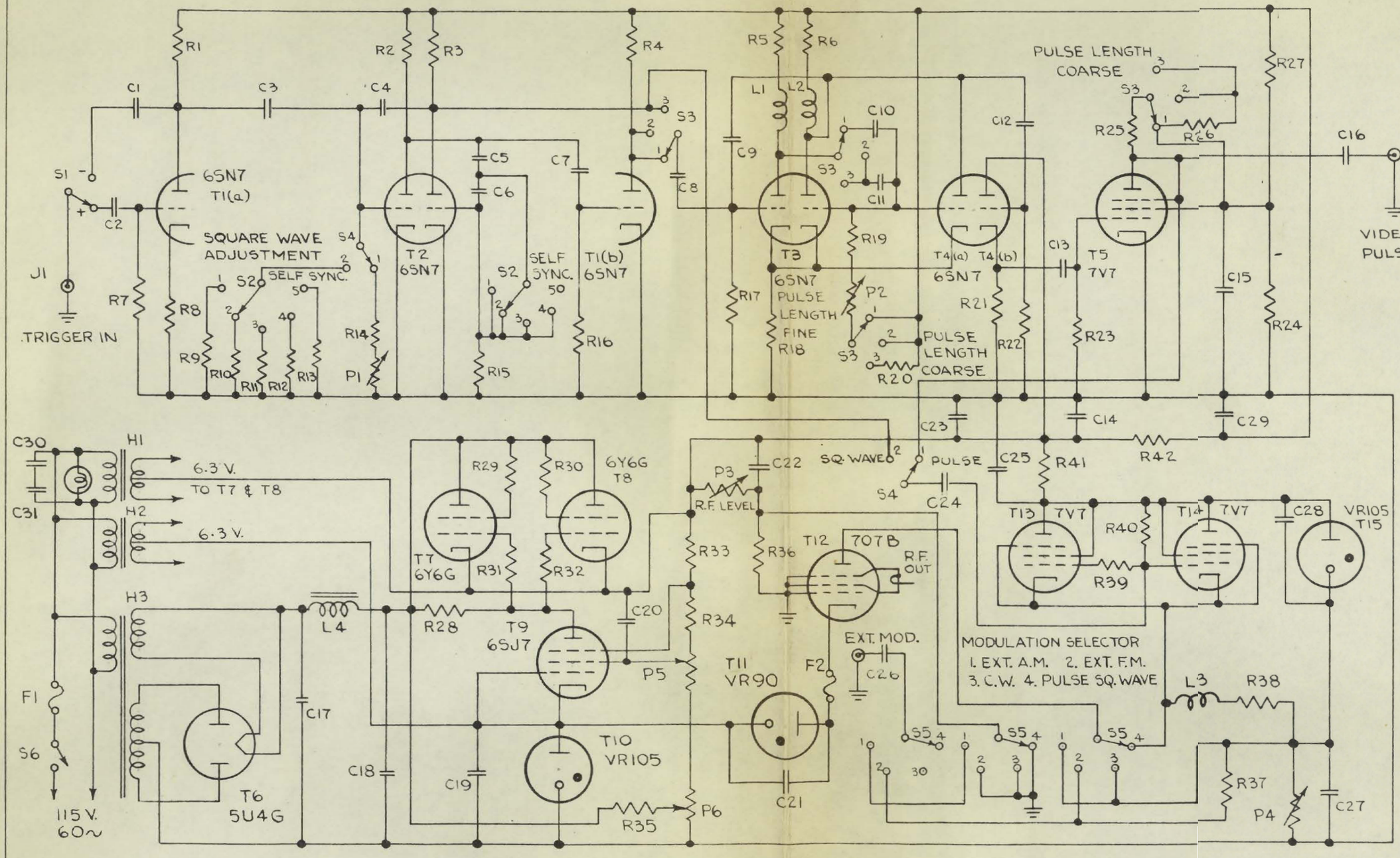

Figure VI
Signal Generator

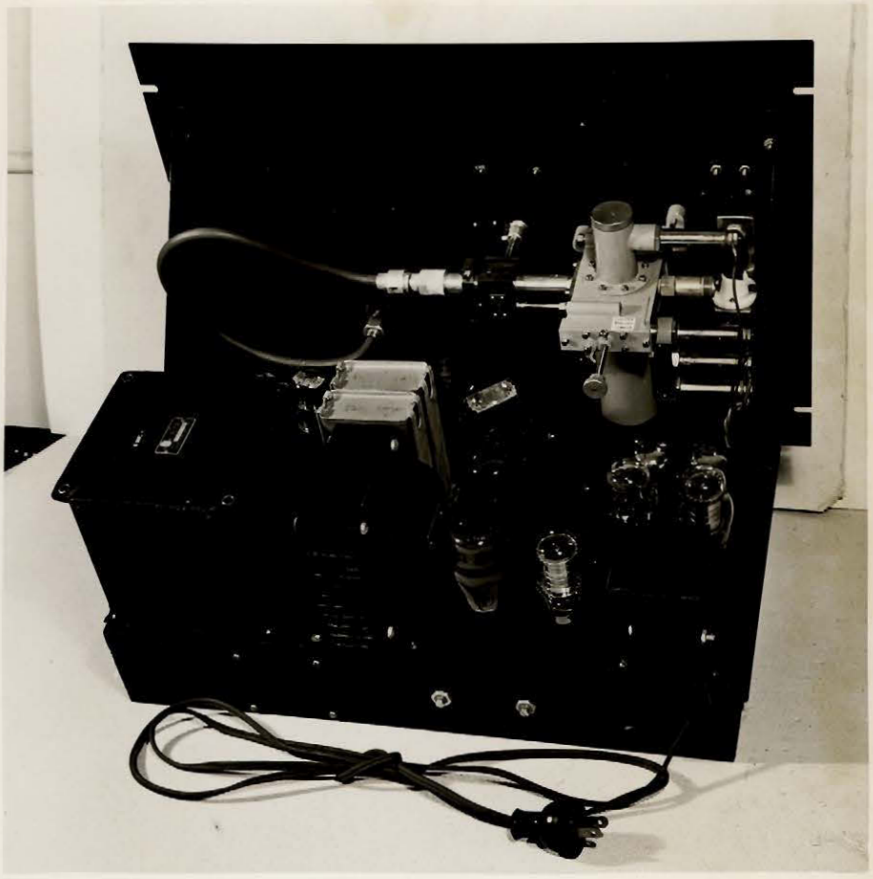

Figure VII
Signal Generator

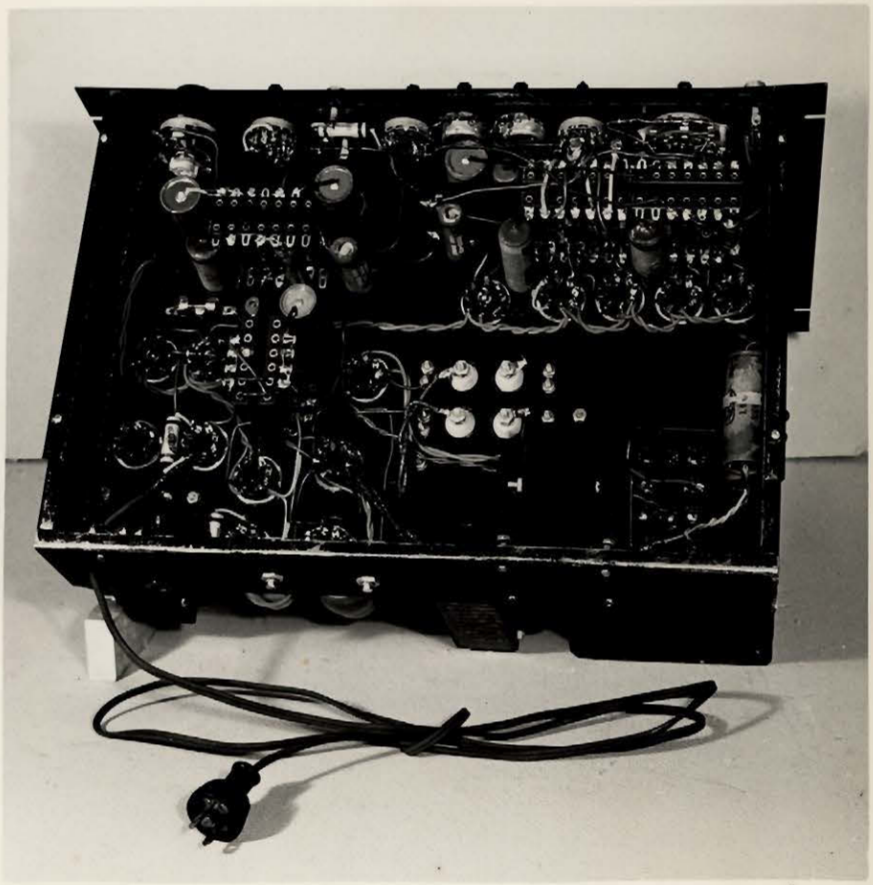

Frequency and amplitude modulation required that external signals be applied to the reflector and accelerating grid respectively. Pure amplitude modulation could not be obtained because modulating the klystron grid voltage also produced frequency modulation. The r.f. level control also produced small frequency changes by altering the grid voltage.

Square-wave modulation at frequencies from 120 to 2000 cps. could be obtained with external triggering. Self-synchronous square-wave operation was possible at a frequency of about 1800 cps. The pulse modulation circuits could produce pulses ranging in length from 1 to 15 micro-seconds. These pulses could be triggered or obtained under self-synchronous operation at repetition rates from 400 to 4000 cps.

In a signal generator it is often important that the frequency of c.w. and pulsed c.w. operation be the same. The signal generator circuit assured this in the following way. If the signal generator was in c.w. operation, switching the modulation selector to internal modulation (pulse-square-wave) changed the reflector voltage of the klystron to a value at which r.f. oscillations did not occur. The arrival of a pulse from the modulating circuits cut off the modulator tubes and removed the blocking voltage for the duration of the pulse. This left the reflector voltage at its original value, ensuring that the operating frequency was unchanged. This circuit only required that the modulating pulses have sharp edges and amplitudes large enough to cut off the modulator tubes.

III PRECISION CALIBRATION OF THE SIGNAL GENERATOR

Calibration of the output power of the signal generator was necessary before it could act as a source of known available signal power. This involved calibrating its cutoff attenuator using relative power measurements, then taking one absolute measurement of the output power at low attenuation.

Calibration of the Cutoff Attenuator

The first step in the calibration of the signal generator was calibrating the cutoff attenuator. The procedure used, that outlined in reference (11), will now be described. Since only relative attenuation was required, a calibration consisted of a graph of attenuation, referred to an arbitrary zero, as a function of the setting of the attenuator dial.

The calibration was made in two stages. Starting at low attenuation, a calibration was obtained by Method I using a precision audio attenuator as a standard of attenuation. For large attenuation it was necessary to use Method II, which extended the calibration using a standard derived from the curve given by Method I.

Method I.

A block diagram of the circuit used in Method I is shown in Figure VIII. Since the audio-frequency voltage output of the bolometer was proportional to the microwave power dissipated in it, one decibel of attenuation in the microwave circuit was equivalent to two decibels in the audio circuit. The audio attenuator was adjusted so that

Figure VIII

Circuit for Calibration by Method I

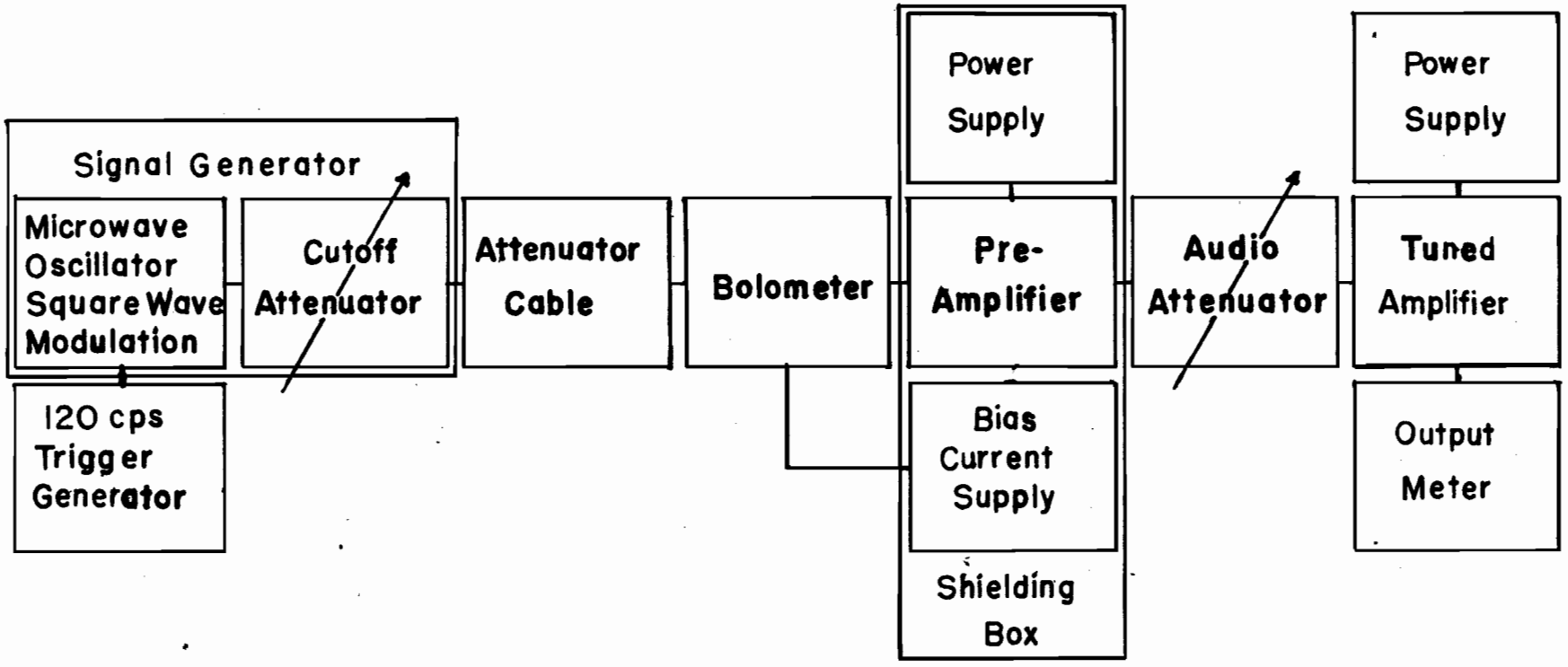

with the cutoff attenuator set at 10 dial divisions, the chosen zero level of attenuation, the output meter deflection was five divisions. Calibration data were obtained by changing the audio attenuation in steps increasing by one decibel and noting the altered settings of the cutoff attenuator required to recover the initial output signal. After each reading the attenuators were reset to ensure that no drift had occurred during the measurement.

This procedure was valid if the following conditions were fulfilled:

(1) noise in the output of the system was negligible,

(2) leakage coupling between any two of the circuit components was negligible,

(3) the preamplifier was linear,

(4) the bolometer was a square-law detector, and

(5) the cutoff attenuator operated into a load with a constant impedance of 50 ohms, the characteristic impedance of the attenuator cable.

The above conditions will now be considered.

(1) The objections to noise in the system were twofold. Noise limited the useful sensitivity of the apparatus by obscuring the signal. Noise delivered to the audio attenuator also produced an output signal that was a function of the audio attenuator setting. If noise had been an appreciable fraction of the output signal, considerable error would have resulted. The noise output was low, in spite of high amplification in the system, because a sharply tuned amplifier was used after the audio attenuator instead of a

wide-band amplifier. This can be easily understood by examining equation 11 which is restated here.

$$N = kT\bar{F}BG(f_o)$$

For amplifiers with the same noise output and noise figure, the product of gain and noise bandwidth is a constant. It follows that a selective amplifier can have a much higher gain than a wide-band amplifier before the noise output reaches an undesirable level. The noise in the system was sufficiently small that with zero decibels in the audio attenuator, the noise output caused a deflection of about three divisions on the output meter.

(2) The microwave oscillator was checked for leakage by turning the signal generator on when the cutoff attenuator was adjusted for maximum attenuation and the audio attenuator for minimum attenuation. A slight increase in signal output was noted which varied only slightly with the cutoff attenuator setting, evidence of a small amount of leakage. The audio signal due to leakage was about 30 decibels below the smallest signal power used in calibrating the attenuator. The maximum error this could have caused would have been 0.2 decibels in the audio system. The corresponding error in the calibration of the cutoff attenuator was 0.1 decibels.

A test was also made to check for leakage across the audio attenuator. An audio oscillator and microvolter replaced the bolometer and microwave circuit in Figure VIII. The effect of inserting 6 decibels at various attenuator

levels was noted when the initial output meter reading was 10.0 divisions. Results of the test are shown in the following table.

TABLE I

Test for Leakage Coupling across Attenuator

Attenuator Settings Decibels		Output Meter Readings Divisions	
Initial	Final	Initial	Final
0	- 6	10.0	6.0
-10	-16	10.0	5.9
-20	-26	10.0	5.7
-30	-36	10.0	5.7
-40	-46	10.0	5.7
-50	-56	10.0	5.7
-60	-66	10.0	5.7
-70	-76	10.0	5.7
-80	-86	10.0	5.7
-90	-96	10.0	5.7
-100	-106	10.0	5.7

The data in Table I show that leakage across the attenuator was negligible, but that noise produced errors if attenuator settings below 20 decibels were used.

(3) The circuit used in the latter part of (2) was also used to check the linearity of the preamplifier. With the audio attenuator at zero decibels, the signal from the audio oscillator was adjusted to produce a deflection of 10 divisions on the output meter. The attenuator setting was increased in steps of 10 decibels while increasing the input signal likewise. The results appearing in the following table show that noise affected the output reading when the audio attenuator was set below 10 decibels, and that nonlinearity in the preamplifier occurred when the signal was increased 100 decibels.

TABLE II

Linearity Test for Preamplifier

Microvolter Setting at Input of Preamplifier	Attenuator Setting at Output of Preamplifier	Output Meter Reading
Decibels	Decibels	Divisions
0	0	10.0
10	- 10	9.9
20	- 20	9.9
30	- 30	9.9
40	- 40	9.9
50	- 50	9.9
60	- 60	9.9
70	- 70	9.9
80	- 80	9.9
90	- 90	9.9
100	-100	9.8
110	-110	8.4

(4) In general bolometers cannot be considered to be square-law detectors, that is, their voltage output is proportional to the square of their voltage input. A close approximation to square-law response is possible, however, if only small signals are to be detected. Deviations from square-law response would have caused differences between calibrations made at different power levels. The data in Table III show that for calibrations made at levels differing by 8 decibels, no differences greater than 0.1 divisions (0.06 decibels) were observed.

TABLE III

Comparison of Calibrations Obtained at Different Signal Levels

Decibels Above 10 Dial Divisions	DIAL DIVISIONS	
	8 Decibels Att.Cable	16 Decibels Att.Cable
6.0	0.6	0.6
4.5	3.0	3.0
3.0	5.2	5.2
1.5	7.6	7.5
0	10.0	10.0
-1.5	12.2	12.2
-3.0	14.6	14.6
-4.5	16.9	17.0
-6.0	19.2	19.2
-7.5	21.7	21.7

TABLE IV

Calibration Data for Cutoff Attenuator at 10.5 Cm.

Obtained by Method I.

Decibels Above 10 Dial Divisions	Dial Divisions	Decibels Above 10 Dial Div.	Dial Divisions
6.0	0.6	-6.5	20.0
5.5	1.4	-7.0	20.6
5.0	2.2	-7.5	21.6
4.5	3.0	-8.0	22.2
4.0	3.8	-8.5	23.0
3.5	4.5	-9.0	23.8
3.0	5.2	-9.5	24.5
2.5	6.0	-10.0	25.3
2.0	6.8	-10.5	26.2
1.5	7.6	-11.0	26.9
1.0	8.5	-11.5	27.6
0.5	9.0	-12.0	28.4
0.0	10.0	-12.5	29.3
-0.5	10.8	-13.0	29.9
-1.0	11.5	-13.5	30.7
-1.5	12.2	-14.0	31.5
-2.0	13.0	-14.5	32.3
-2.5	13.8	-15.0	33.1
-3.0	14.6	-15.5	33.9
-3.5	15.4	-16.0	34.7
-4.0	16.2	-16.5	35.5
-4.5	16.9	-17.0	36.2
-5.0	17.7	-17.5	37.0
-5.5	18.5	-18.0	37.8
-6.0	19.2	-18.5	38.7

(5) It was necessary to load the output of the cutoff attenuator with the impedance for which a calibration was desired, because at low attenuation the power extracted from the oscillator cavity depends on the impedance at the attenuator output. This is due to the fact that when the attenuator loop is moved near the iris in the oscillator cavity, the iris is shunted by a load whose impedance approaches that at the output of the attenuator. The load impedance could be varied by adjusting the tuning of the bolometer mount (Figure IX), a stub-matched length of coaxial waveguide containing the bolometer in the centre conductor. The bolometer mount was matched for maximum power dissipation in the bolometer with 25 decibels of attenuator cable isolating the mount and the cutoff attenuator. All the calibration data were obtained without changing this tuning, but with 8 or 16 decibels of attenuator cable replacing the 25 decibel length. Since both calibrations agreed within 0.06 decibels, particularly for the low attenuation settings (see Table III), the load at the iris in the oscillator cavity must have remained constant throughout the calibrations.

Amplifier Details for Method I

A preamplifier, tuned amplifier, and pulse generator were built to supply the apparatus for Method I.

The preamplifier (Figure X) had one high gain stage operating into a cathode follower to provide a low output impedance. This was done because the input impedance of the audio attenuator was 600 ohms. The output of the attenuator

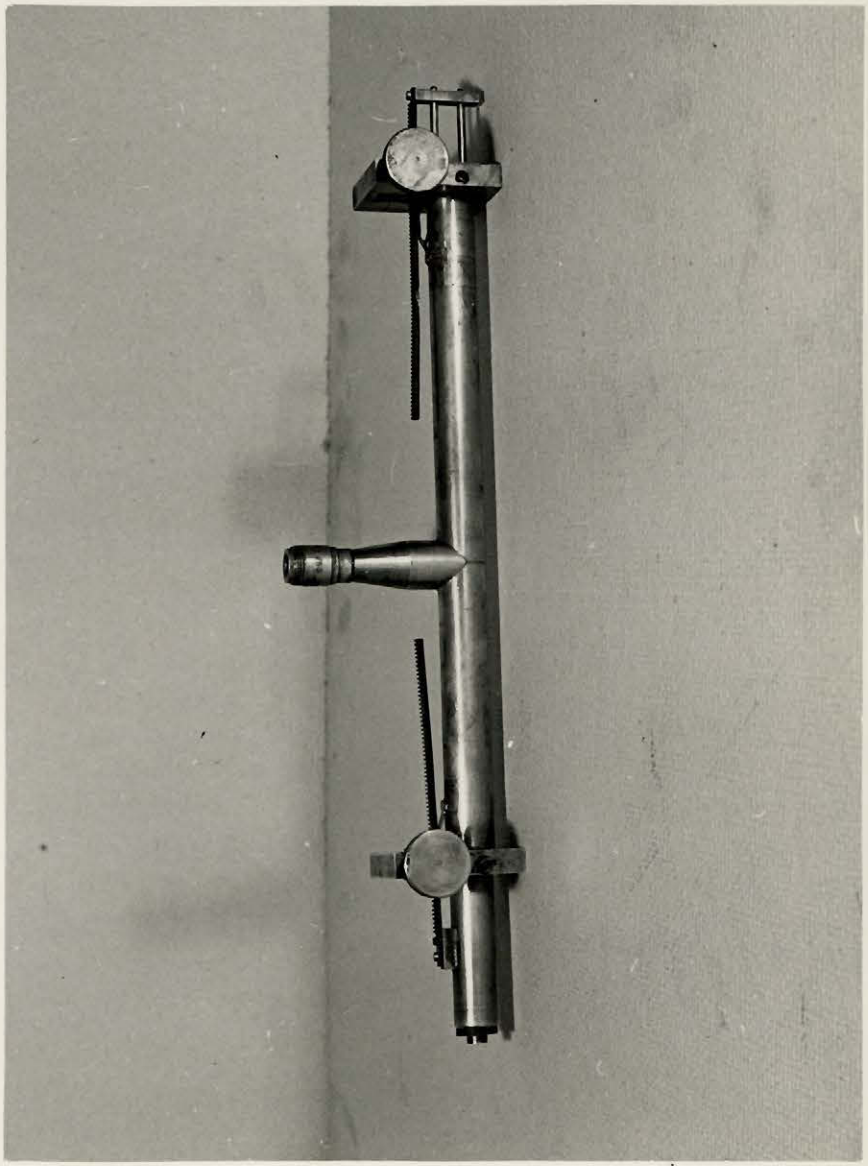

Figure IX

Figure X

Pre-Amplifier Circuit

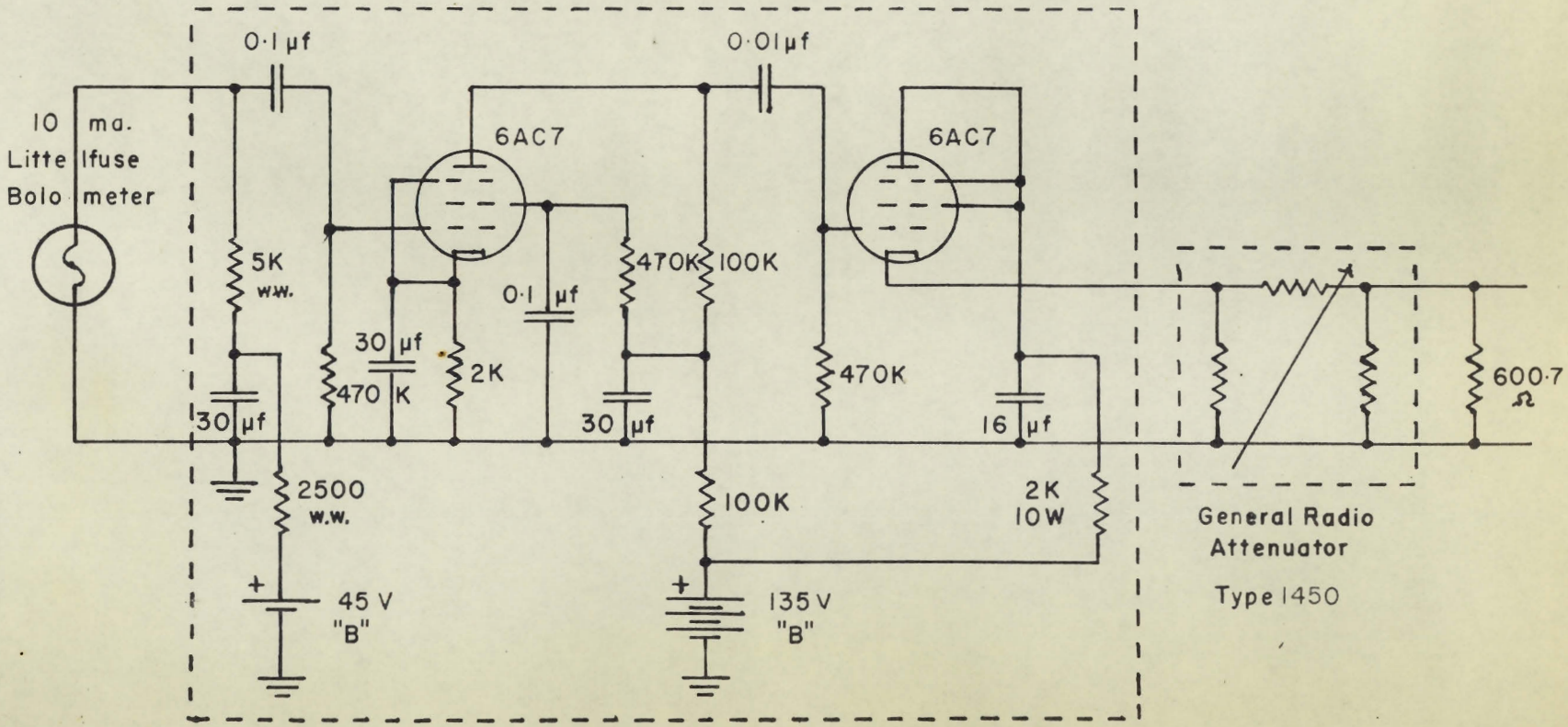

Figure XI

Tuned Amplifier

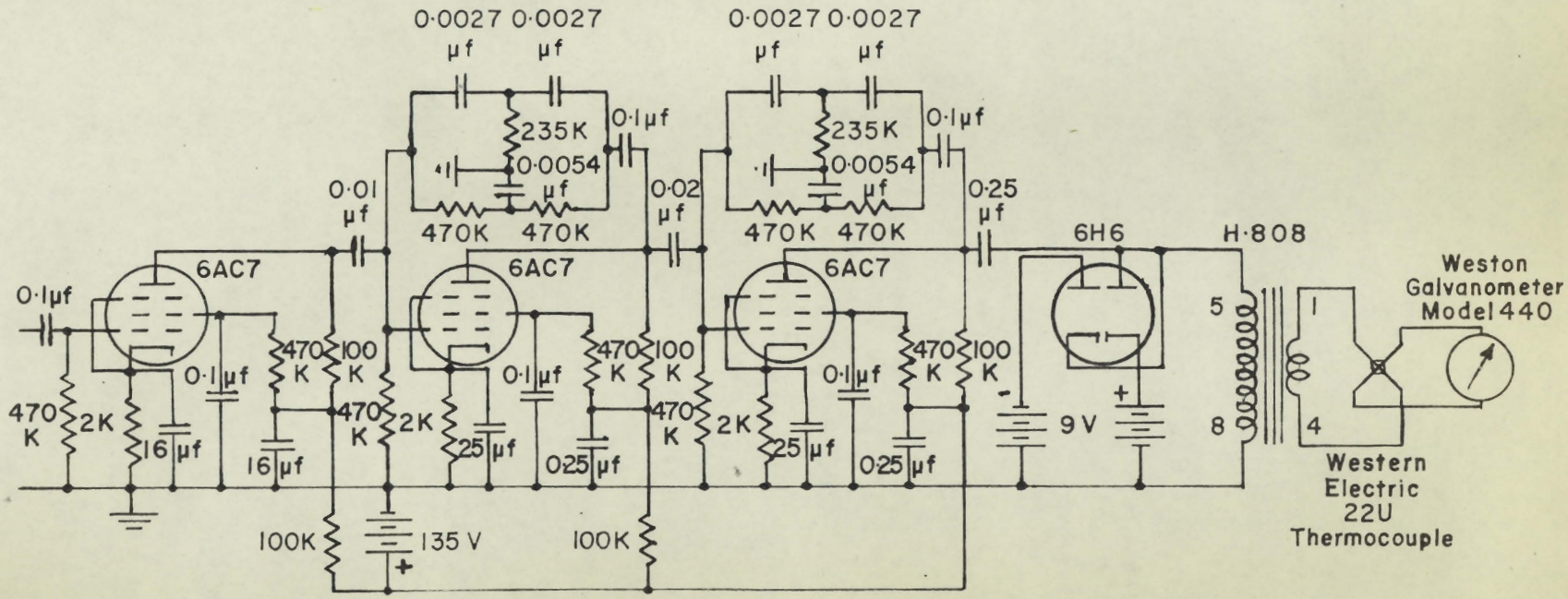

was accurately matched to establish the input impedance of the attenuator. This avoided errors which could have been introduced by an input or output mismatch varying with the attenuator setting. The bolometer, a 10 milliampere Littelfuse, was biassed with about six milliamperes d.c. from a high impedance source. The Littelfuse resistance at this current was about 250 ohms.

The tuned amplifier (Figure XI) was a three stage high gain amplifier using twin-t's for selectivity. A twin-t permits the passage of signals of all frequencies except those in a very narrow band. The twin-t's were therefore used to provide negative feedback at all frequencies except at 120 cps., the frequency at which the signal generator was modulated. The bandwidth of the amplifier was about 5 cps. A signal limiting circuit was necessary at the output to protect the thermocouple from burnout.

The twin-t components were chosen to satisfy the conditions

$$R_1R_2C_3 = (R_1 + R_2)(C_1 + C_2)\,R_3 \qquad (15)$$

and

$$4\pi^2f^2C_1C_2(R_1 + R_2)\,R_3 = 1 \qquad (16)$$

where the symbols refer to the components in Figure XII and f is the frequency at which the impedance between the terminals A and B becomes infinitely large ((12) Section 10.0). If A and B are connected to the grid and plate of a tube there will be no feedback at this frequency. To avoid computation and measuring many components, the conditions

Figure XII

Twin-T Circuit

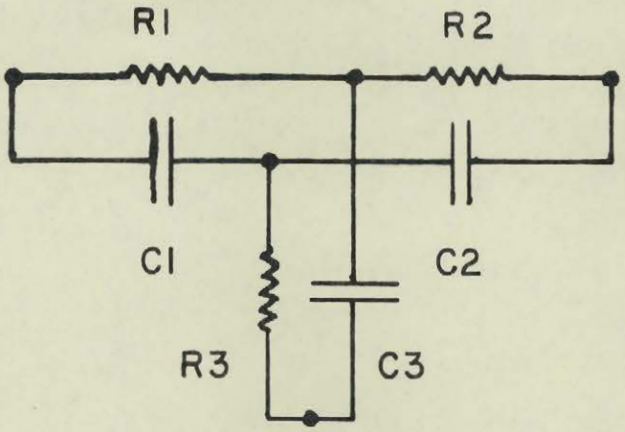

Figure XIII

120 Cps. Trigger Generator

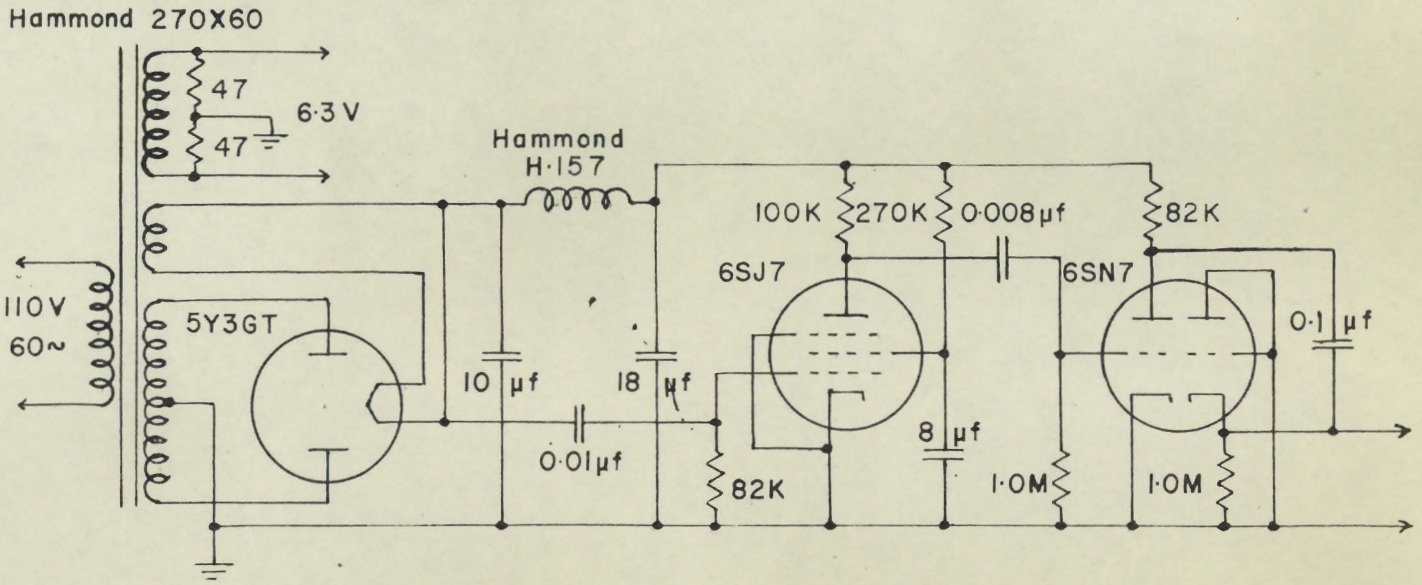

$2\,fCR = 1$, $R_1 + R_2 = 2R$, $C_1 + C_2 = 2C$, $R_3 = R/2$, and $C_3 = 2C$ were satisfied. Since R_1 and C_1 were also chosen to be within 5% of R and C respectively, the conditions $R_1R_2 = R^2$ and $C_1C_2 = C^2$ necessary to satisfy equations 15 and 16 were automatically satisfied to within $\frac{1}{4}$% not allowing for errors in the measured values of the components. All components were measured to an accuracy of 1%.

The preamplifier and tuned amplifier required shock-absorbing bases. A heavy wooden box lined with copper screening was used to provide electrical shielding and protection from acoustic shock for the preamplifier and all its batteries. These measures provided sufficient protection as all readings were stable and easily reproduced.

The pulse generator (Figure XIII) used the full wave rectifier as a frequency doubler to obtain a triggering pulse with a stable repetition rate of 120 cps. This was necessary because the sharp tuning of the tuned amplifier made the response of the audio circuit vary with small frequency changes.

Method II

Figure XIV is a block diagram of the circuit used to extend the calibration curve of a cutoff attenuator. The receiver was matched for maximum power output with approximately 50 decibels of attenuator cable between the signal generator and the microwave receiver.

Figure XIV
Apparatus for Calibration
by Method 2

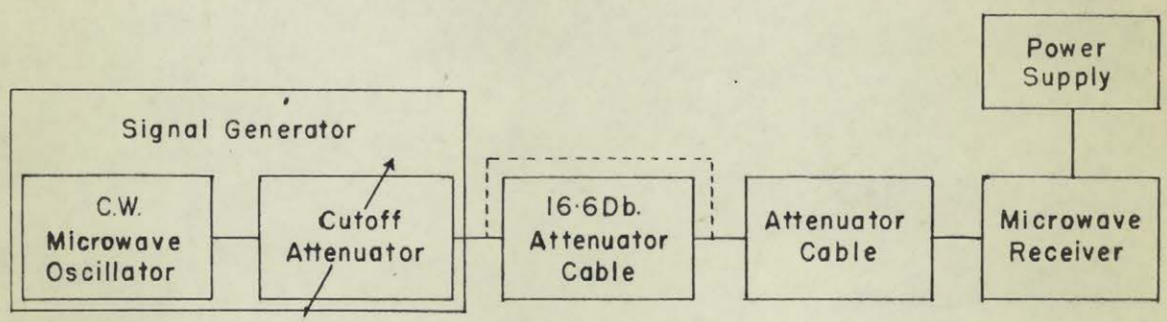

The calibration procedure first involved setting the cutoff attenuator at some level and noting the receiver output reading. Twenty feet of attenuator cable next to the signal generator were then removed and the attenuator setting necessary to recover the original output reading was noted. The original conditions were then reproduced to see that no drift occured during the measurement. This procedure was repeated with a succession of settings of the cutoff attenuator. When the initial and final attenuator settings were within the range calibrated by Method I, a mean value of 16.6 decibels was obtained for the attenuation of the cable. When only one setting was within the calibrated range, it was then possible to obtain the setting of a point 16.6 decibels above it. The complete calibration was therefore achieved by a series of extensions of the calibrated portion of the curve. The data from which the calibration was extended follow in Table V.

TABLE V

Calibration Data Obtained using Method II

Attenuator Settings

Initial Reading	Reading after Removal of 16.6 Decibels	Initial Reading	Reading after Removal of 16.6 Decibels
Dial Divisions			
20.0	45.8	55.0	80.7
25.0	50.7	60.0	85.6
30.0	55.7	65.0	90.6
35.0	60.6	70.0	95.7
40.0	65.6	75.0	100.7
45.0	70.9	80.0	106.0
50.0	75.7		

The chief difficulty in taking measurements was caused by changes in attenuation produced by moving the centre conductor of the cable when plugging and unplugging cable connections. This was partially overcome by arranging the cable so that changing the cable connections did not entail moving more than a few inches of cable. The cable was also supported so that no strains were set up near the connectors. Individual determinations of the attenuation of the twenty foot length of attenuator cable did not differ from the mean by more than 0.15 decibels. The calibration could not be carried further because the signal at the receiver input became too small to be measured accurately.

The microwave receiver used in these measurements will now be described briefly. The receiver (Figure XV) was a superheterodyne receiver using a crystal mixer. A matching cavity at the input allowed the receiver to be matched to a signal source. The local oscillator was a 707B reflex klystron whose operating frequency was adjusted to produce an intermediate frequency of 26 megacycles per second. The i.f. amplifier response produced an output signal proportional to the logarithm of the input signal. The output meter was therefore calibrated linearly in decibels. To avoid changes in the receiver response due to frequency drifts in the system, the intermediate frequency was kept constant by an automatic frequency control circuit. This circuit altered the frequency of the local oscillator to compensate for changes in either the signal generator or local oscillator frequencies. The a.f.c. could not compensate for the frequency change produced by varying the signal generator's

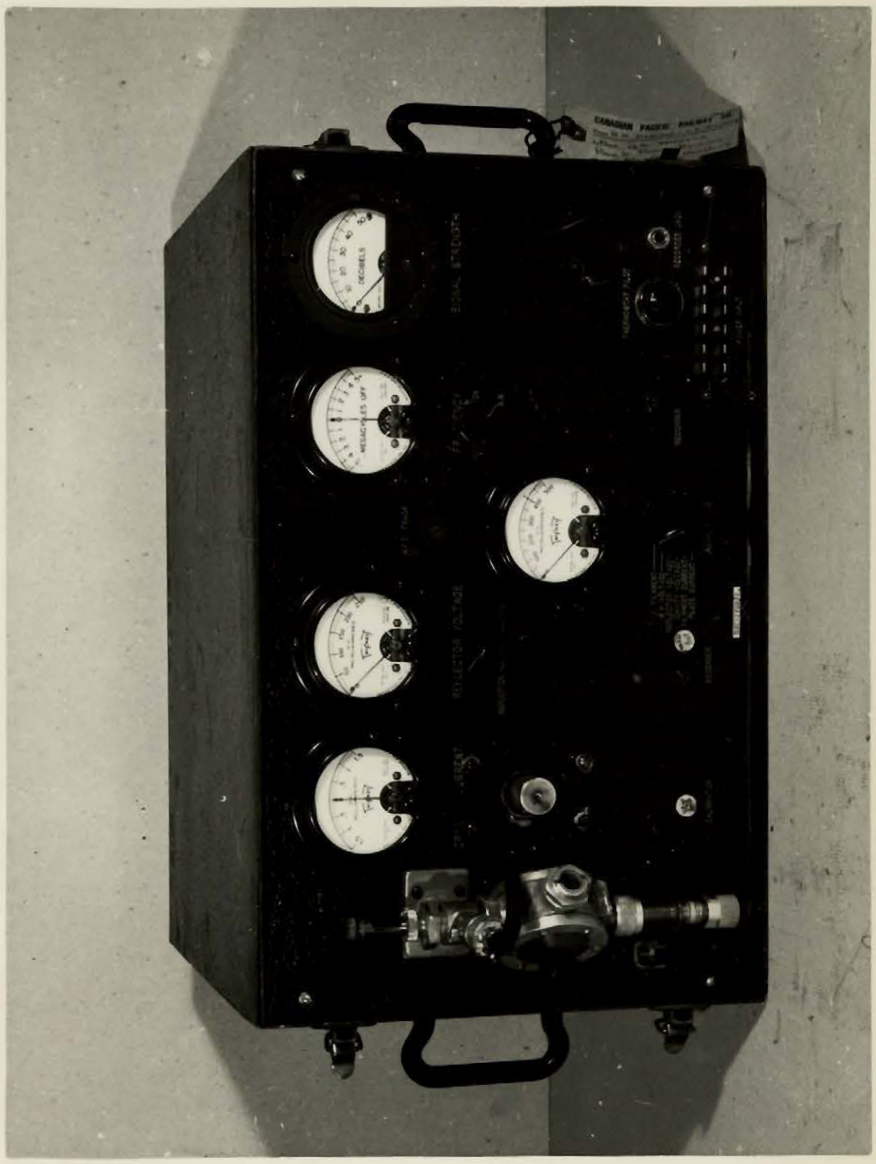

Figure XV

r.f. level control. All measurements were therefore taken at a constant setting of this control.

Results

The calibration curve for the cutoff attenuator is shown in Figure XVI. A comparison of the slope of this graph with that predicted by the gearing of the attenuator loop and equation 14 appears in Table VI.

TABLE VI

Slope of Calibration Curve at 10.5 Cm.

Decibels per Dial Division		
Theoretical	Experimental	Percentage Deviation
0.653	0.648	0.8

The divergence between these results is within the error possible in the calibration. A small amount of this error could be due to the audio attenuator used as a standard. The manufacturer's specifications state that the attenuator components were chosen within ½% of design values, but that the maximum error in any setting would not exceed 1%, (0.044 decibels). The calibration curve of the cutoff attenuator should be accurate to within 0.1 decibels when the calibration was derived using Method I, and within one percent over the range calibrated by Method II. A locking adjustment on the attenuator was set so that the coupling loop could not be moved sufficiently close to the iris for nonlinearity to occur due to the presence of modes

Figure XVI
Calibration of Cutoff Attenuator
at 10.5 Cm.

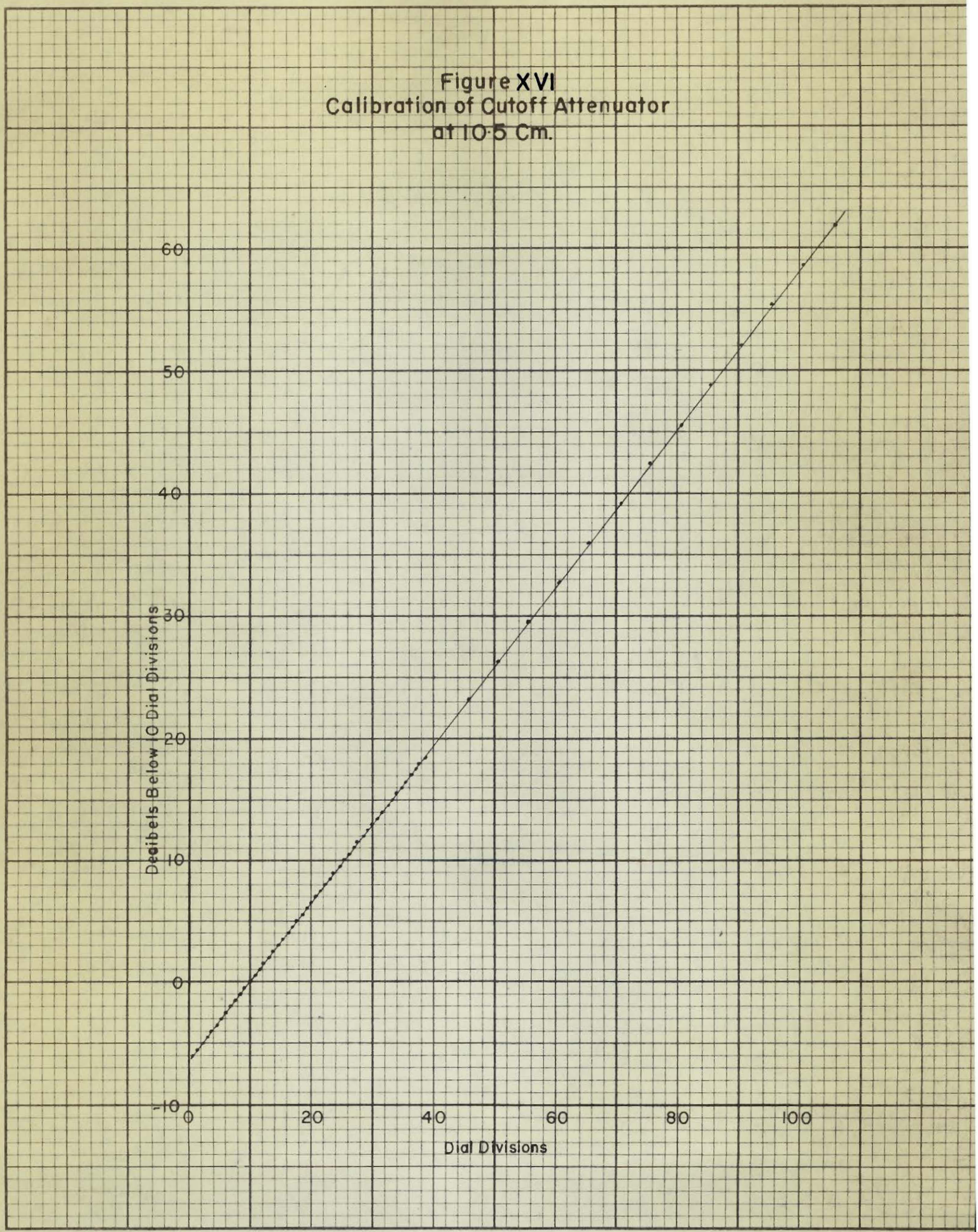

other than the TE_{11} mode, or due to a change in the input impedance of the attenuator. This is the reason the calibration curve was linear over the whole range investigated.

The Absolute Measurement of Available Output Power

Calibration of the cutoff attenuator was the first step in calibrating the signal generator output power. To complete a calibration in terms of absolute power it was necessary to make one absolute measurement of the available output power. This was done at low attenuation. The measurement was made by comparing the heating effects of r.f. and d.c. power. The apparatus for this measurement was a Wheatstone bridge in which one of the arms was a 10 milliampere Littelfuse bolometer. When the bridge was balanced with only direct current through the bolometer, dissipating r.f. power in the bolometer produced a bridge unbalance. Balance could be restored by decreasing the d.c. power supplied to the bridge until the bolometer resistance returned to its original value. The change in d.c. power dissipated in the bolometer was then equal to the r.f. power.

This method can be used only if the heating effects of equal amounts of d.c. and r.f. power are identical. D.c. power is dissipated uniformly throughout a wire, whereas r.f. power is dissipated mainly at the surface because of the skin effect. If the diameter of the bolometer wire is small enough, no temperature gradient will appear across the wire when it is heated with r.f. power. A theoretical treatment in section 3.24 of reference (9) based on this

assumption shows that the d.c. resistance of a bolometer, when heated by r.f. power instead of an equal amount of d.c. power, will be changed by only a fraction of one percent. The bolometer impedance must be carefully matched to that of the signal generator if a measurement of available power is to be made. The bolometer mount and bolometer lead wires must also be lossless if accuracy is to be obtained. Losses in the mount, or errors because the heating effects of d.c. and r.f. power are not comparable, are difficult to measure. The Bell Telephone Laboratories have made measurements with a 1 cm. thermistor mount using as a standard the power indication of a water load. The maximum disagreement was 0.3 decibels (section 3.21, reference (9)). Better agreement would be expected for a comparable bolometer mount at 10 cm. since losses in the mount and in the bolometer lead wires would be smaller.

The absolute power output of the signal generator at any attenuator setting will be a function of the cavity tuning, the reflector voltage, the setting of the r.f. level control, and the length of attenuator cable connected at the output of the cutoff attenuator. The absolute available output power should therefore be measured after these variables have been adjusted in preparation for other measurements.

The discussion of the microwave measuring equipment has now been completed. The rest of this thesis is devoted to a consideration of double-stream amplification, the investigation of which required the construction and calibration of the signal generator.

PART TWO

DOUBLE-STREAM MICROWAVE AMPLIFICATION

I MATHEMATICAL THEORY OF DOUBLE-STREAM AMPLIFICATION

Double-stream amplification is a process, the existence of which has been predicted mathematically. A physical picture of the way in which two electron streams interact to produce a growing space charge wave has not been discovered. For this reason a mathematical treatment of the process will be given, and physical interpretation will be applied only to the results. The theoretical case which will be considered will neglect the problem of coupling power to and from electron streams, and will consider only two interacting electron streams.

The model to be examined consists of two intermingled electron streams infinite in extent and travelling in the X direction of a Cartesian coordinate system. D.c. space charge effects will be neglected and it will be assumed that none of the quantities considered vary in the YZ plane. This theory will only treat the case where the amplitude of a.c. disturbances is small enough that the product of two a.c. quantities can be neglected in comparison with the product of an a.c. and a d.c. quantity. The following symbols will be used with the subscripts 1 and 2 to denote quantities associated with beams 1 and 2 respectively.

These quantities are:

r, the d.c. space charge density,

s, the a.c. space charge density ,

u, the d.c. velocity of the electrons,

v, the a.c. velocity of the electrons,

E, the a.c. electric field intensity,

e/m, the electronic charge to mass ratio, and

$w = (4\pi re/m)^{\frac{1}{2}}$, the plasma frequency.

The equations of motion of the two beams are

$$dv_1/dt + u_1 dv_1/dx = Ee/m$$

and

$$dv_2/dt + u_2 dv_2/dx = Ee/m.$$

E is common to both beams. The equation of continuity applied to each beam separately is

$$r_1 dv_1/dx + u_1 ds_1/dx + ds_1/dt = 0$$

and

$$r_2 dv_2/dx + u_2 ds_2/dx + ds_2/dt = 0.$$

The a.c. space charge densities are related to the a.c. electric field intensity by the equation

$$dE/dx = 4\pi (s_1 + s_2).$$

Assuming that all a.c. quantities vary with time and distance as

$$q = q_o \exp j(wt + Px) ,$$

the five equations previously mentioned become

$$j(w + Pu_1)v_1 = Ee/m,$$

$$j(w + Pu_2)v_2 = Ee/m,$$

$$Pr_1 v_1 + (w + Pu_1)s_1 = 0,$$

$$Pr_2v_2 + (w + Pu_2)s_2 = 0$$

and $$jPE = 4\pi(s_1 + s_2) \quad .$$

In order that the five unknowns in these five linear equations may have non-zero values which are solutions of these equations, it is necessary for the determinant of their coefficients to vanish. When the determinant is expanded and equated to zero, the following equation results:

$$(w_1/(w + Pu_1))^2 + (w_2/(w + Pu_2))^2 = 1. \qquad (17)$$

Equation 17 is a quartic in P, hence an a.c. disturbance propagated in the electron streams can be composed of four waves, one for each root of the equation. The types of waves corresponding to different types of P are of great interest. A real value of P corresponds to a sinusoidal wave propagated in the streams at a constant amplitude. If P is zero, standing waves exist in the stream. If P is complex, a wave is propagated in the stream with an amplitude varying exponentially with the distance travelled. Since all the coefficients in the quartic are real, if one complex P exists, the complex conjugate of P also exists. If P_i is the imaginary part of the complex root P, a wave must exist with an amplitude increasing with distance as exp $(P_i x)$, and another wave must exist with an amplitude decreasing with distance as exp $(-P_i x)$. An exponentially increasing wave will eventually become large in comparison with the other waves which can exist in the system. The gain in energy of such a wave as it propagates in the stream

will be P_i nepers per unit length. Expressed in decibels, the gain will be

$$G = 8.686\, P_i \tag{18}$$

decibels per unit length. The conditions governing the existence of a complex P are therefore of special interest. These conditions and the resulting values of P_i have been investigated by Nergaard (3) in terms of the parameters

$$A = (w_1 w_2)^{\frac{1}{2}}/(wS) , \tag{19}$$

where $$S = \tfrac{1}{2}((u_1/u_2)^{\frac{1}{2}} - (u_2/u_1)^{\frac{1}{2}}),$$

$$B = ((w_1 w_2)/(w_2 u_1))^{\frac{1}{2}} , \tag{20}$$

and $$C = 2/3 - A^2(B^2 + 1/B^2)/6 .$$

The condition for the existence of complex roots is

$$A^4 > 2C^3 .$$

The value of the imaginary part of the propagation constant was calculated in terms of a dimensionless gain factor X defined by the equation

$$X = ((u_1 u_2)/(w_1 w_2))^{\frac{1}{2}} P_i . \tag{21}$$

The gain of the increasing wave is then

$$G = 8.686((w_1 w_2)/(u_1 u_2))^{\frac{1}{2}}\, X \tag{22}$$

decibels per unit length. Graphs of X as a function of A for several values of B can be found in Nergaard's article (3).

In using this analysis to determine the beam parameters of a double-stream amplifier, it is more convenient to express the beam velocities and plasma frequencies in terms of beam voltages and current densities. The following

relations then result:

$$w_n/u_n = 309\ j_n^{\frac{1}{2}}/V_n^{\frac{3}{4}},$$

$$w_n = 1.85 \times 10^{10} j_n^{\frac{1}{2}}/V_n^{\frac{1}{4}},$$

$$B = (j_1/j_2)^{\frac{1}{2}}(V_2/V_1)^{\frac{3}{4}}, \qquad (23)$$

$$A = \frac{3.70 \times 10^{10}\ j_1^{\frac{1}{2}}/V_1^{\frac{1}{4}}}{wB\ ((V_1/V_2)^{\frac{1}{2}} - 1)},$$

and $$G = 2.68 \times 10^{3} X j_1^{\frac{1}{2}}/(BV_1^{\frac{3}{4}}), \qquad (25)$$

where j_n is the current density in beam n in amperes per square cm., and V_n the beam voltage in volts. The current density may be eliminated from equations 24 and 25 to give the equation

$$G = 7.26 \times 10^{-8}\ wAX(1/V_2^{\frac{1}{2}} - 1/V_1^{\frac{1}{2}}) \qquad (26)$$

The conditions for the optimum value of X are $A = 2/3^{\frac{1}{2}}$, and $B = 1$.

To determine whether or not the conditions for double-stream amplification will require physically realisable current densities and voltages, examine a system operating at 10.7 cm. (1.76×10^{10} radians / sec.) with beam voltages of 500 and 400 volts. At conditions for optimum X, this system would have a gain of 3.89 decibels per cm. Current densities of 74.8 and 53.4 milliamperes/ sq.cm. would be required for the 500 and 400 volt beams respectively. These voltages and current densities can be obtained. If the growing wave were propagated 25 cm., it would then be expected to increase 97 decibels.

The theoretical gain previously calculated could not be expected in an experimental tube because edge effects associated with electron streams of finite breadth were not

considered. The effects of space charge and incomplete mixing of electron streams have also been neglected, as have transverse electric fields in the beams. The fact that the theoretical treatment applies only to signals of small amplitude can also limit the gain.

II CONSTRUCTION OF A DOUBLE-STREAM AMPLIFIER TUBE

A block diagram of a tube using a growing wave to produce an amplified signal is shown in Figure XVII. The source of two electron streams must deliver two well mixed beams of electrons of the desired voltages. In addition the current densities should be easily variable if the conditions for double-stream amplification are to be satisfied. The input coupling system serves to excite the growing wave in the electron streams. The growing wave then proceeds through the interaction space where it increases in size until it reaches the output coupling. There the wave excites a magnified signal in the output coupling system. The efficiency of the coupling systems was not considered in the theoretical treatment previously given. This is another potential source of losses in an experimental tube.

A helix or resonant cavity are convenient coupling systems. If a helix is used at the input, modulation of the electron streams is achieved by choosing the dimensions of the helix so that the axial velocity of propagation of the signal in the helix is approximately the velocity of one of the electron beams. The same criterion determines the dimensions of the output helix which is excited by the

Figure XVII

Block Diagram of a Double Stream Amplifier

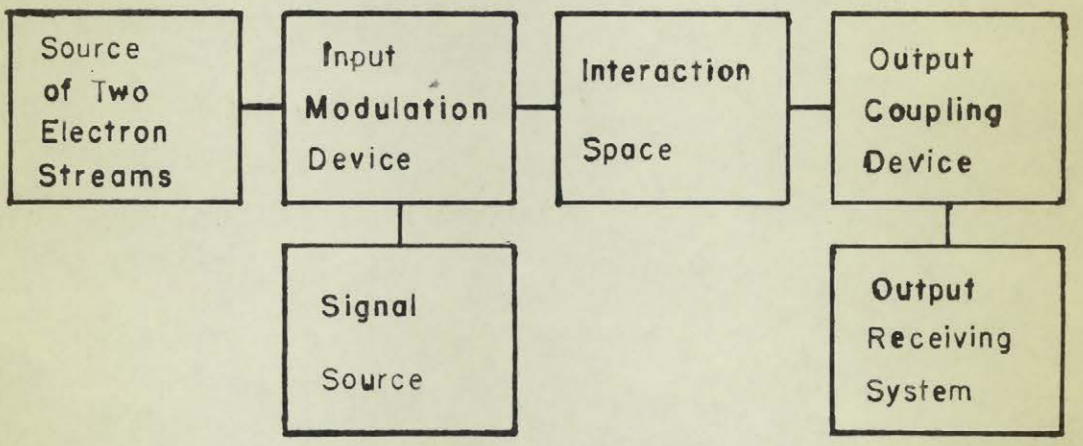

electron streams. If a resonant cavity is used, the electrons are directed through closely-spaced parallel grids in a re-entrant portion of the cavity. The input signal produces an electric field between the grids and so modulates the electron streams. The time of transit of an electron between the grids must be small in comparison with the time for one cycle of the incoming signal if efficient modulation is to result. This may be achieved by using high voltage electron beams. This, however, cannot be continued indefinitely since the current density requirement of the beams increases with increased beam voltages.

The interaction space consists of an evacuated region in which the growing wave increases in amplitude before entering the output coupling system. Since the gain of the tube is governed by the length of this space, it is desirable that the interaction space be as long as possible. The length of this space is limited by the defocussing and mutual repulsion of the electrons in the beams, and the difficulty in directing the beams through the output coupling system. To keep the beams compact and to send them through the output coupling system, a strong magnetic field is maintained in the direction of the output coupling system.

The previous paragraphs in this section dealt with general aspects of double-stream amplifier tubes. The tube constructed by G.A. Harrower will now be briefly described. A complete description of this tube and problems

associated with its design can be found in reference (13). A photograph of the tube appears in Figure XVIII. The tube used a very efficient electron gun system in which two intermingled electron streams were produced by projecting the current from one gun through the system producing the second beam. The currents could be varied by changing the filament temperatures or the voltages of control electrodes. Resonant cavities were used at both the input and output of the tube. The diameter of the metal tube bounding the interaction space was chosen small enough that the tube was a waveguide well beyond cutoff at 10.7 cm., the proposed signal wavelength. This avoided direct coupling between the input and output. Solenoids for magnetic focussing in the interaction space are not shown in Figure XVIII, but appear in Figure XIX. The meters in Figure XIX were those used to indicate the currents and voltages in the electron gun system. Since brass was used in the tube construction, and sealing wax in making vacuum seals, the tube could not be permanently sealed and required continuous pumping when it was in operation. The vacuum system used was a three-stage oil diffusion pump operating into a mechanical forepump. The diffusion pump was capable of producing an ultimate vacuum of 10^{-7} mm. of mercury.

III RADIO-FREQUENCY MEASUREMENTS

The signal generator was used to supply power to the tube at a wavelength of 10.7 cm. The receiver used in the calibration of the cutoff attenuator measured the

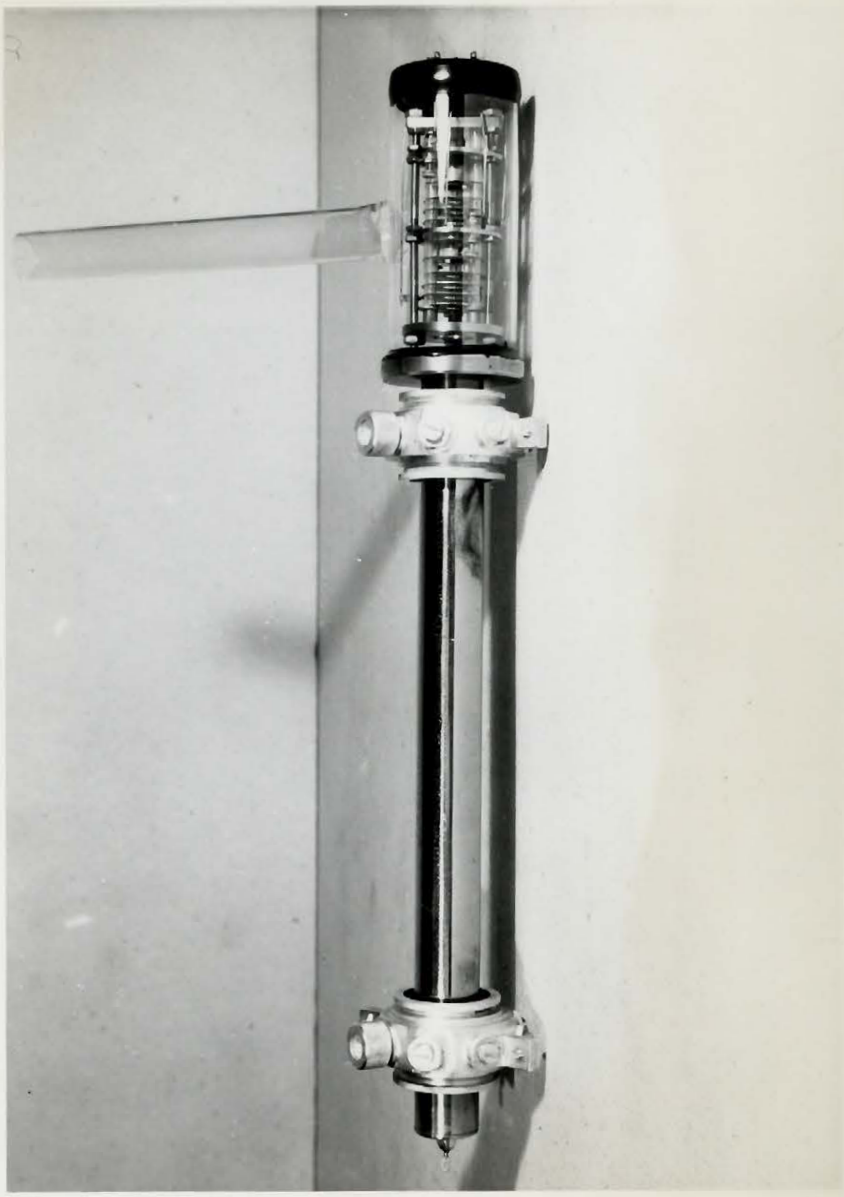

Figure XVIII

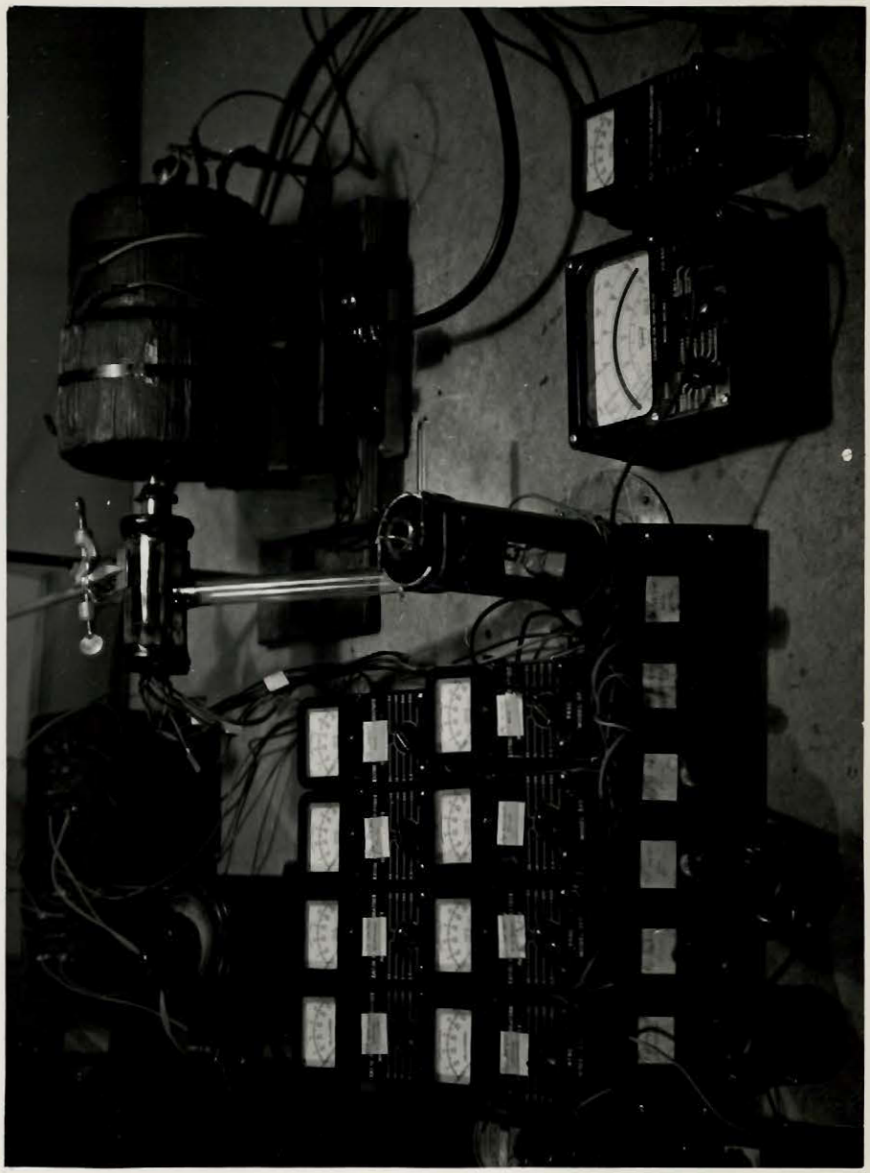

Figure XIX

output power of the tube. Matching adjustments at the receiver input were made with approximately 30 decibels of attenuator cable connecting the receiver and signal generator. When the tube was inserted in the circuit, the input was connected to the signal generator through approximately 20 decibels of attenuator cable. Ten decibels of attenuator cable connected the output of the tube to the receiver. This ensured that a mismatch at the output of the tube could not affect the receiver tuning. Before operating the tube it was necessary to tune the input and output cavities. Tuning consisted of screwing threaded tuning plugs into the cavities. To detect the optimum tuning, one of the tuning plugs was removed and replaced by a coupling loop which was connected to the receiver. The tuning plugs were then adjusted for maximum power transfer between the input and output coupling loops. The cavities were tuned separately in this manner and then tuned in series. Following this the electron beams were turned on and the tuning adjusted once more for maximum response. In all cases the maximum occurred when the tuning plugs were screwed in as far as possible. Since the maximum obtained was not sharp, and it was not possible to make adjustments beyond the maximum, it was most probable that resonance was not obtained. It follows that a considerable loss in the amplification of the signal could have occurred.

After the cavity tuning had been checked with both beams operating, the output signal obtained with single beams was investigated. With either beam operating alone,

maximum beam current produced the maximum output. The signal output did not vary with small changes in beam voltage provided the beam current remained constant. When both beams operated simultaneously, the behaviour of the output signal was entirely different.

The output was first investigated when the beam voltages and the current in the fast beam were kept constant. The current in the slow beam was varied by adjusting the appropriate filament voltage. As the current was increased, the output stayed near the value obtained for a single beam until a critical current was reached. After this the signal rose quickly to a maximum. Further increase in the current eventually resulted in a slight decrease in signal. If the currents were adjusted for maximum response, decreasing the current in the fast beam slowly decreased the signal output. The output was still above that from a single beam when the current was only a few microamperes.

The current densities at which an output reading was obtained could only be estimated. This was shown by previous tests made with the electron gun system operating at a pressure of about 4.5×10^{-4} mm. of mercury. At this pressure the electron beams were visible due to the ionization produced by the electrons. The fast beam did not fill the final aperture in the gun system. Increasing the current in the fast beam caused the beam to spread slightly. The current from the slow beam filled the final aperture

in the gun system, but was not uniformly distributed over this aperture, judging the current density by the intensity of the light produced by the beam. The values of the current densities were also doubtful because progressive spreading of the beams must have occurred in spite of the magnetic field in the interaction space. Assuming that the final aperture in the gun system was filled uniformly, the maximum current densities available at the output of the electron gun system were 6.8 and 15 ma./sq.cm., corresponding to currents of 0.47 and 1.1 ma. in the fast and slow beams respectively.

After the effect of varying the current densities was found, the beam currents were adjusted for maximum signal output and the beam voltage ratio was varied. The output decreased gradually but passed through a series of small ripples of two to three decibels amplitude. The ripples were not predicted by the mathematical theory of double-stream amplification. The theory, however, neglected the presence of three additional waves, one attenuated and two of constant amplitude, which could have been excited in the electron streams. (See paragraph following equation 17). Varying the beam voltages would have altered the phases of these waves relative to that of the growing wave. This could have produced the ripples observed.

The maximum reproducible signal amplitude is recorded in Table VII. This table also gives the results obtained with each of the electron beams operated separately using the same beam voltages and currents. These readings were

easily reproduced. A much higher output was obtained on one occasion when the output meter read 29 decibels. This reading, however, demanded a critical adjustment of the beam parameters and could not be recaptured.

TABLE VII

Response of Receiver			
Beam One	Beam Two	Both Beams	Tube Removed from Circuit
Output Meter Readings in Decibels			
6	11	19	46

IV DISCUSSION OF RESULTS

The data in Table VII show that there was a net loss of signal in the tube even when the maximum signal output occurred. This does not mean that double-stream amplification did not occur, since losses greater than any double-stream gain may have occurred in the cavity coupling systems. If it is postulated that there was no double-stream amplification, but that the signals obtained with the separate beams were unchanged when the beams operated together, it can be shown that the output signal observed could not have been obtained. Under conditions where double-stream amplification did not exist and the beams did not load one another, the maximum output possible from beams 1 and 2 operating together would be $(V_1 + V_2)$,

where V_1 and V_2 are the output voltages from beams 1 and 2 operating alone. Since the receiver output meter was calibrated in decibels, the calculation of $(V_1 + V_2)$ requires some consideration. Designate the zero decibel reference voltage by V_r. Since the decibel readings of the outputs of beams 1 and 2 were 6 and 11 decibels respectively,

$$20 \log V_1/V_r = 6 \quad \text{or} \quad V_1 = V_r\, 10^{0.30},$$

$$\text{and} \quad 20 \log V_2/V_r = 11 \quad \text{or} \quad V_2 = V_r\, 10^{0.55}.$$

The decibel reading of the voltage $(V_1 + V_2)$ would then be

$$20 \log (V_1 + V_2)/V_r = 14.9$$

decibels. Since the maximum signal observed when both beams were operated together was 19 decibels, unless double-stream amplification existed, there was a considerable discrepancy to be explained. The calculation of this discrepancy is conservative when it is considered that the worst possible phase relationship between the voltages was assumed. If the voltages had been out of phase, the decibel reading would have been

$$20 \log (V_2 - V_1)/V_r = 3.8$$

decibels. G.A. Harrower (Appendix I, reference (13)) calculated that the phase difference was approximately 72° at the end of the interaction space. This calculation was based on the assumption that the phase velocity of a wave in a modulated stream of electrons is the same as the d.c. velocity of the electrons.

The results in the previous paragraph indicate the existence of an amplifying effect not present in the single streams of electrons. The qualitative behaviour of the signal output furnishes additional proof of the existence of double-stream amplification. The observations of the r.f. output as the current densities in the beams were altered agree with the predicted behaviour shown in Figure XX. The graphs in Figure XX were plotted from data calculated using equations 25, 24 and 26, and a graph of X as a function of A for various values of B. The graph can be found in reference (3). Referring to Figure XX and recalling the estimates of the maximum current densities available, it is seen that the current densities were not large enough to satisfy the conditions for large gains.

If the ripples observed in the output when the beam voltage ratio was varied were caused by unattenuated waves propagated in the electron streams, the gain of the growing wave can be estimated from the amplitude of the ripples. Near the maximum output the peak to peak amplitude of the output ripple was about two decibels. If the growing and unattenuated waves were excited with equal initial amplitudes, the gain in the growing wave was about 20 decibels. The corresponding theoretical prediction of the gain can only be crudely estimated because of the uncertainty in the effective current densities, but was probably about 30 decibels.

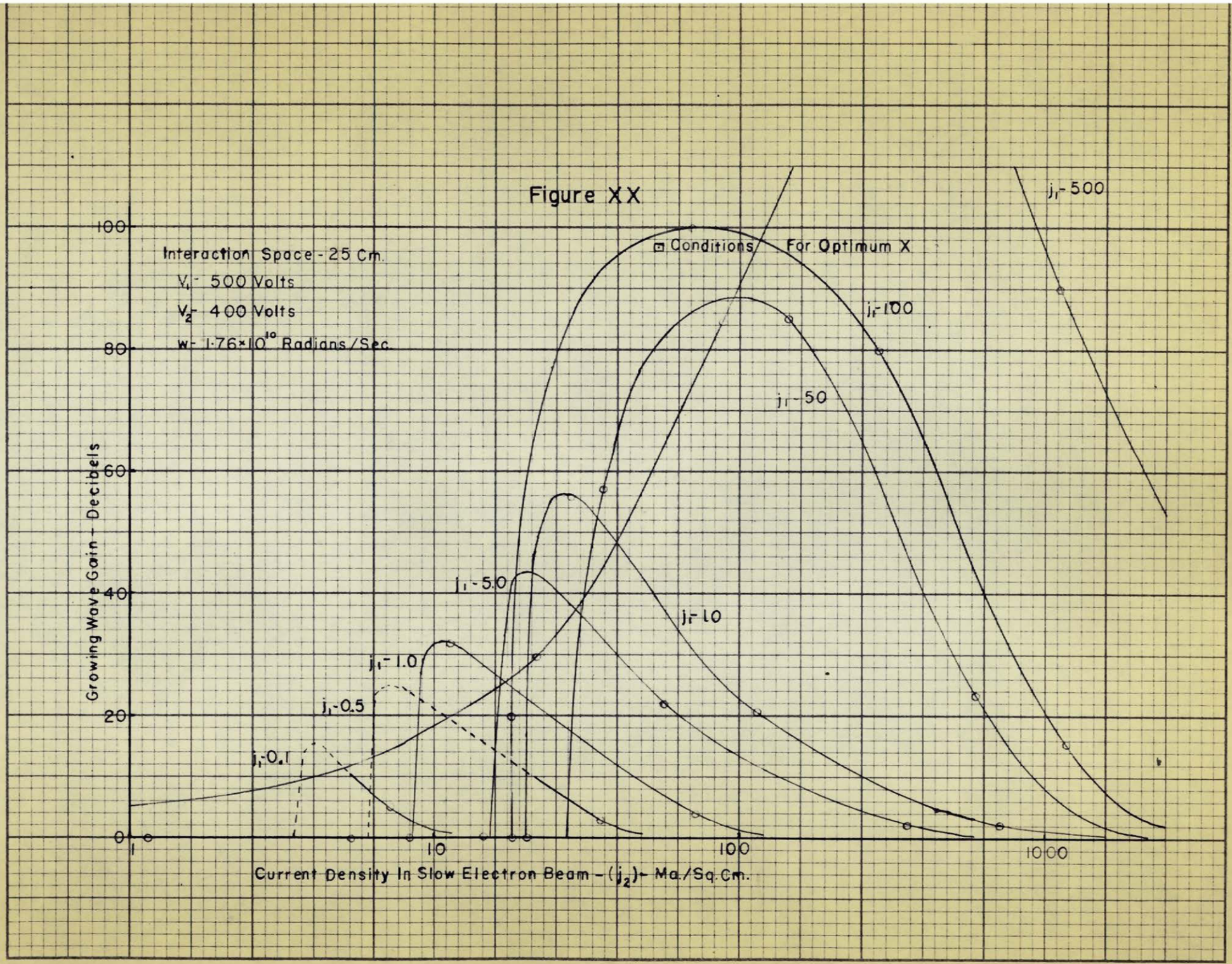
Figure XX
Interaction Space - 25 Cm.
V_1 - 500 Volts
V_2 - 400 Volts
w - 1.76×10^10 Radians/Sec.
⊡ Conditions For Optimum X
j_1 - 500
j_1 - 100
j_1 - 50
j_1 - 10
j_1 - 5.0
j_1 - 1.0
j_1 - 0.5
j_1 - 0.1
Growing Wave Gain - Decibels
0
20
40
60
80
100
1
10
100
1000
Current Density In Slow Electron Beam - (j_2) - Ma./Sq. Cm.

V LOSSES IN THE SYSTEM

Attention has been previously focussed on the gain of the growing wave in the tube without much consideration of the gain of the tube as a whole. While the tube gain can be increased if the conditions for greater gain of the growing wave are satisfied, an increased overall gain can be obtained even if the beam parameters governing the amount of double-stream amplification are kept constant. If the beam currents are doubled without changing the current densities, the gain of the growing wave is the same, but the voltage output of the tube is doubled and the tube gain is increased by 6 decibels. A tube operating with low currents but high current densities could thus have a low gain even if a high growing wave gain was achieved. Reference to Figure XX shows, however, that the current densities are the more important factor since an increase in the current densities available will produce as great or greater gains than a corresponding percentage increase in the currents available. Obviously one of the reasons for the large insertion loss of the tube was the inability of the electron gun system to supply beams with either high currents or high current densities. Other reasons for the insertion loss of the tube can be found by examining the r.f. circuitry in the tube construction.

No provisions were made for impedance matching at either the input or output cavities. The impedance measured across a loop coupling into a cavity is a high

resistance when the cavity is resonant, and a high reactance when the cavity is off resonance. In either case the impedance would be large in comparison with the 50 ohm. resistance of the input and output cables. It is therefore very probable that large losses occurred due to mismatches at the input and output cavities. This could have been eliminated by installing tuning sections at the input and output of the tube.

The design of the cavities was another factor which contributed to the losses in the system. The cavities had been originally designed to resonate at 10.7 cm. The modifications made when they were converted for use in the tube, particularly the large increase in the area of the closely spaced cavity grids, increased the capacitive loading of the cavities and lowered their resonant frequency. This explains why tuning necessitated screwing the tuning plungers into the cavities as far as possible. The ratio of the volume to the surface area of the cavities was decreased by the tuning, hence the Q of both cavities was lowered. The tuning plugs also caused considerable distortion of the fields inside the cavities, which must have resulted in poor coupling to the input and output loops. The fact that resonance was almost certainly not obtained has already been mentioned as a reason for losses in the system. The time of transit of the electrons between the cavity grids was responsible for a small decrease in the amplification of the signal, since the beam coupling

coefficients were less than unity. This loss was calculated to be 0.82 decibels at both the input and output cavities. (See Appendix II, reference (13)).

SUMMARY

A microwave signal generator satisfactory for making signal and noise measurements on a double-stream amplifier tube was built and its absolute available output power precisely calibrated. Factors in the design and construction of the signal generator were discussed. The precision calibration of the signal generator involved calibrating a cutoff attenuator and measuring the absolute power output of the signal generator at a low attenuation setting. The cutoff attenuator was calibrated to within 0.1 decibels over a 25 decibel range by a substitution method using a precision audio attenuator in an audio system with a square-law detector. The calibrated range was extended to 65 decibels by a second substitution method using a microwave attenuation standard evaluated by the above audio method. The absolute power measurement was made with a bolometer bridge.

The theory of double-stream amplification was reviewed and the construction of double-stream amplifier tubes discussed. The r.f. output of an experimental double-stream amplifier was examined, using the signal generator as a signal source at a wavelength of 10.7 cm. The objective of the investigation, to observe double-stream amplification, was achieved. The observations agreed qualitatively with theoretical predictions.

The double-stream amplifier could not be used as a practical amplifier since it had a net insertion loss.

The insertion loss occurred partially because the conditions for high double-stream gains could not be satisfied, and partially because of losses due to the design of cavity couplings in the tube and the lack of impedance matching at the input and output of the tube. These factors are being considered in an improved double-stream amplifier which is now under construction.

ACKNOWLEDGMENTS

The author wishes to thank all those who have assisted in this project and in the preparation of this thesis, especially Mr. G. Bekefi and Mr. G.A. Harrower who, with the author, comprised a group investigating double-stream amplification under the direction of Professor G.A. Woonton. The microwave receiver used in the r.f. measurements was loaned by the National Research Council, Ottawa, through the generous co-operation of Dr. G.A. Miller.

REFERENCES

(1) HAEFF, A.V. The Electron Wave Tube - A Novel Method of Generation and Amplification of Microwave Energy. Proc. I.R.E. 7:4-10 January 1949.

(2) HOLLENBERG, A.V. Experimental Observations of Amplification by Interactions Between Two Electron Streams. Bell Syst. Tech. Jour. 28:52-8 January 1949.

(3) NERGAARD, L.S. Analysis of a Simple Model of a Two-beam Growing Wave Tube. R.C.A.Rev. 9:585-601 December 1948.

(4) PIERCE, J.R. and HEBENSTREIT, W.B. A New Type of High Frequency Amplifier. Bell Syst. Tech. Jour. 28:33-51 January 1949.

(5) PIERCE, J.R. Double Stream Amplifiers. Proc. I.R.E. 37:980-85 September 1949.

(6) PIERCE, J.R. Increasing Space Charge Waves. Jour. Appl. Phys. 20:1060-66 1949.

(7) FRIIS, H.T. Noise Figures of Radio Receivers. Proc. I.R.E. 32:419-22 July 1944.

(8) WOONTON, G.A. Preliminary Report on Signal to Noise Measuring Methods at 10 cm. P.R.A.68 February 1943.*

(9) MONTGOMERY, C.G. Technique of Microwave Measurements, #11 M.I.T. Radiation Laboratory Series. McGraw-Hill Book Co.,Inc., New York 1947.

* This report may be obtained by applying to the National Research Council, Radio Branch, Ottawa.

(10) STRATTON, J.A. Electromagnetic Theory.
McGraw-Hill Book Co. New York 1941

(11) ANONYMOUS. Report on the Calibration of a Wave-Guide Attenuator at Wave-Lengths in the Neighbourhood of 10 cm.
U.W.O.Report No.20. April 1943.*

(12) VALLEY, S. and WALLMAN, H. Vacuum Tube Amplifiers.
#18 M.I.T. Radiation Lab. Series.
McGraw-Hill Book Co. New York 1948.

(13) HARROWER, G.A. A Double-Stream Amplifier for Micro-Wave Frequencies.
M.Sc. Thesis, McGill University.
August 1950.

* This report may be obtained by applying to the National Research Council, Radio Branch, Ottawa.

BIBLIOGRAPHY

Double-Stream Amplification

(1) Haeff, A.V. The Electron Wave Tube - A Novel Method of Generation and Amplification of Microwave Energy.
Proc. I.R.E. 7:4-10. January, 1949.

(2) Hollenberg, A.V. Experimental Observations of Amplification by Interactions Between Two Electron Streams.
Bell Syst. Tech. Jour. 28:52-8. January 1949.

(3) Nergaard, L.S. Analysis of a Simple Model of a Two-Beam Growing Wave Tube.
R.C.A.Review 9:585-601. December, 1948.

(4) Pierce, J.R. and Hebenstreit, W.B. A New Type of High Frequency Amplifier.
Bell Syst. Tech. Jour. 28:33-51. January 1949.

(5) Pierce, J.R. Double-Stream Amplifiers.
Proc. I.R.E. 28:980-85. September, 1949.

(6) Pierce, J.R. Increasing Space Charge Waves.
Jour. Appl. Phys. 20:1060-66. 1949.

(7) Discussion on "The Electron Wave Tube".
Proc. I.R.E. July, 1949.

(8) Hollenberg, A.V. The Double-Stream Amplifier.
Bell Lab. Records. 27:290-2. 1949.

Microwave Measurements.

(9) Montgomery, C.G. Technique of Microwave Measurements.
#11 M.I.T.Radiation Laboratory Series.
McGraw-Hill Book Co. New York. 1947.

(10) Friis, H.T. Noise Figures of Radio Receivers.
Proc. I.R.E. 32:419-22. July, 1944.

The following reports may be obtained by applying to the National Research Council, Radio Branch, Ottawa.

(11) Bleaney, B., Griffiths, J.H.E. and Roaf, D. The Design of Signal Generators and Measurement of the Merit of Receivers at 9.1 cms.
C.L. Misc. 1. Clarendon Lab.

(12) Report on the Calibration of a Wave-guide Attenuator at Wavelengths in the Neighbourhood of 10 cms.
U.W.O. Report #20. April, 1943.

(13) Special Report on Signal to Noise Measurements on Receivers.
September 29, 1941.
M.I.T.Report X 10 Section IV Report 5S.

(14) Breazeale, W.M. Noise Measurements on Microwave Converters. September, 1942.
M.I.T. Report 61-7.

(15) Woonton, G.A. Preliminary Report on Signal to Noise Measuring Methods at 10 cm.
February, 1943. P.R.A. 68.

(16) Special Report on the Littelfuse Bolometer.
October 28, 1941.
M.I.T.Report. Section VII - RF Rep. 45.

(17) Breazeale, W.M. A 10-20 Centimeter Bolometer.
August 26, 1942. 61-6.
M.I.T. Report 6185.